DIPLOMARBEIT
Master´s Thesis

INVESTIGATION OF THE RUNOUT MODELING OF DEBRIS FLOW USING DAN3D

UNTERSUCHUNGEN ZUR MODELLIERUNG VON MURGÄNGEN MITTELS DAN3D

ausgeführt zum Zwecke der Erlangung
des akademischen Grades eines Diplom-Ingenieurs

unter der Leitung von

Univ.Prof. Dipl.-Ing. Dr.techn. Rainer Poisel
E220 Institut für Ingenieurgeologie

und

Assistant Prof. Dipl.-Ing. Dr.techn. Alexander Preh
E220 Institut für Ingenieurgeologie

eingereicht an der Technischen Universität Wien
Fakultät für Bauingenieurwesen

von

Pichler Lukas BSc
Simon Denk-Gasse 10/3
1090 Wien, Österreich

Wien, im Juni 2011

Acknowledgment

I would like to thank everybody who helped me writing this thesis.

It was a good experience working in the Institute of Geotechnics where I was provided with everything I needed and even more. Many thanks to the project assistant Dipl.-Ing. Kurt Mair am Tinkhof for all the help on GIS software issues.

I want to address many thanks to Assistant Prof. Dipl.-Ing. Dr.techn. Alexander Preh who found always time discussing some major or minor problems with me. His interest in modeling and in the outcome of my thesis was a big help for me and an additional source of motivation.

Special thanks to Univ.Prof. Dipl.-Ing. Dr.techn. Rainer Poisel who supervised this thesis and was always seeing the big picture of this work and which topics should be focused on.

I need to thank the governmental department "Wasserschutzbauten" for providing me with all available event data, specially Dr. Omar Formaggioni and Dr. Pierpaolo Macconi.

Last but not least I need to thank my family. Because of their help I was not only able to focus on my study but also to have time for my personal growth.

Abstract

Debris flows are a big threat to mountainous regions. Predicting future events can help to mitigate disasters and provide important information for more efficient mitigation measures. In order to predict debris flows by numerical models, numerous back-calculations of different events need to be performed in order to create a parameter dataset.

This thesis analyses the capabilities of the continuum dynamic model DAN3D modeling debris flows, and its performance to back-calculate the 2002 debris flow event "Seefeldbach" (Italy). The program can simulate the runoff of granular material over a complex 3D terrain, including the influence of its internal strength, material entrainment along the path and six different basal friction rheologies.

In order to show the influence of the input parameters, sensibility analyses were performed using an idealized topography. For this analysis, the Voellmy basal friction rheology was used. By varying the input parameters, dependencies on relevant results (e.g runout distance) were found. The results show that the unit weight has no influence on the results and that the friction coefficient f has the biggest influence on the model.

The back-analysis of the "Seefeldbach" event showed the urgent need for more incident data and that the correctness of the GIS data is of great importance. It was possible to reproduce the pre-event topography only with a low degree of accuracy, and therefore some error was introduced into the model.

The back-analysis was performed using both the Voellmy and frictional rheology. Due to the introduced errors, not all features of the runout behavior could be reproduced. The deposit position and its heights could be simulated quite accurately by both rheologies. The model which uses the Voellmy rheology gave the best results, and is therefore recommended for modeling similar events.

Kurzfassung

Murgänge stellen eine große Gefahr für gebirgige Regionen dar. Die Vorhersage solcher Prozesse kann dazu beitragen, das Schadenspotenzial zu verringern und Schutzbauten effizienter zu gestalten. Um jedoch solche Vorhersagen mittels numerischen Modellen treffen zu können, sind noch zahlreiche Rückrechnungen verschiedenster Murgänge nötig, um einen geeigneten Datensatz für die Eingabeparemeter zu erlangen.

Diese Diplomarbeit untersucht die Möglichkeiten des kontinuummechanischen Modells DAN3D, an Hand des Murgangereignisses "Seefeldbach" (2002, Italien), Muren numerisch zu simulieren. Das Programm kann das Fließen von granularem Material über ein komplexes 3D Gelände modellieren und berücksichtigt den Einfluss der internen Festigkeit, Materialakkumulierung entlang des Abflusses und sechs verschiedene Rheologien des Fließwiderstands.

Um den Einfluss der Eingabeparameter verstehen zu können, wurde eine Sensibilitätsanalyse an einem idealisierten Gelände durchgeführt. Dabei wurde die Voellmy-Rheologie benützt. Durch diese Studie konnten Abhängigkeiten zu relevanten Resultaten (z.B. Auslauflänge) gefunden werden. Es zeigte sich, dass die Wichte des Murmaterials keinen Einfluss auf die Ergebnisse hat, sowie dass der "friction coefficient" f den größten Einfluss auf die Rechenergebnisse ausübt.

Die Rückrechnung des "Seefeldbach"-Ereignisses zeigte den dringenden Bedarf an detailierteren Ereignisdokumentationen und dass die Genauigkeit der GIS-Daten wesentlich ist. Da die Topografie nur ungenau reproduziert werden konnte, konnten die Ergebnisse nur in gewissen Schwankungsbereichen angegeben werden.

Bei der Rückrechnung dieses Ereignisses wurde die Voellmy und Frictional Rheologie benützt. Durch die Ungenauigkeit der Geländetopografie konnte das Abflussverhalten nicht exakt nachgebildet werden. Die Lage und Höhe der Endablagerung wurden aber recht gut rekonstruiert. Das Modell, welches die Voellmy-Rheologie beinhaltet, lieferte die beste Anpassung an die Realität und kann deshalb empfohlen werden, um ähnliche Prozesse zu modellieren.

Contents

Chapter 1

Introduction

Debris flows are a dangerous threat which could be mitigated by predicting their impact on urbanized areas and on infrastructure. Modeling software which can predict the runout deposit would make it possible to design mitigation measures which stop the debris premature, or to change the urban planning in order not to locate infrastructure in its runout and deposit area.

DAN3D (McDougal, 2006) is a 3D extension of the software DAN (Hungr, 1995) which was developed to model extremely rapid landslides. The determination of parameters is calibration based and therefore needs back-calculations in order to evaluate the exact model parameters.

The aim of this master thesis is to back-analyze the 2002 "Seefeldbach" debris flow event. The main equations on which this model is based on will be analyzed, in order to get a better understanding of the calculation procedure. A sensibility analysis of the DAN3D parameters will give answers to the correlation between those parameters and important results (e.g. runout length). Combining this information, an accurate back-analysis of the "Seefeldbach" event can be performed and should give answers to the suitability of this software to model alpine debris flows.

Chapter 2

Theoretical background of DAN3D

DAN3D is a continuum dynamic modeling software for the analysis of extremely rapid landslides (McDougal, 2006). This includes rock avalanches, debris avalanches, debris flows and flow slides.

It was developed in the course of the PhD thesis of McDougal (2006) and is a 3D extension of the existing 2D model DAN-W (Hungr, 1995). DAN3D is based on a meshless, Lagrangian numerical method which is adapted from the Smoothed Particle Hydrodynamics. This discretization aims at solving the depth averaged equations of motion for an "equivalent fluid". The "equivalent fluid" approach replaces the heterogeneous and complex material with an equivalent fluid which approximates the bulk properties of the real material (Hungr, 1995). Figure 2.1 shows a comparison of the prototype material and the equivalent fluid.

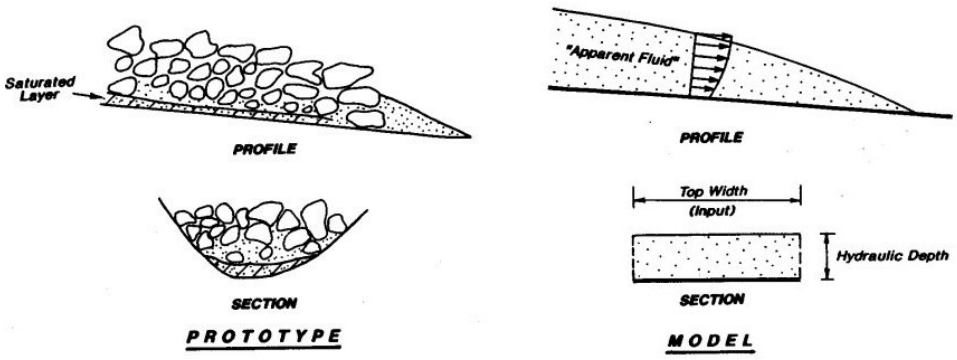

Figure 2.1 – Heterogeneous material compared with an equivalent (apparent) fluid after Hungr (1995)

2.1 Implementation issues

Modeling debris flow is challenging because there are many macroscopic and microscopic effects influencing it. The author of the DAN3D code (McDougal, 2006) implemented the most important rapid landslide properties in an accurate, practicable, physically comprehensible and efficient way.

2.1.1 3D terrain

3D terrain has a significant influence on the runout dynamics. There can be sudden redirections, surface irregulations or confinements. All these topography changes lead to changes in the internal stress and therefore in changes of the basal shear stress. This can change the direction of the flow, its velocity and height distribution.

2.1.2 Influence of internal stress

Internal stress distribution

Debris flows behave similar to fluids. Therefore the basic assumption of the internal stress distribution is hydrostatic and isotropic. Due to the fact that debris flows consist not only of water, but to an essential part of earth material, this assumption needed to be improved. Earth materials can resist shear strains by developing shear stresses. Sassa (1988) and Hutter and Savage (1988) were the first to incorporate such a material behavior into a dynamic landslide model. The shear stresses are incorporated by the Rankin earth pressure theory. This theory is widely used in geotechnical engineering and was tested and improved by many authors (Terzaghi et al., 1967).

The Rankine earth pressure theory uses the Mohr-Coulomb failure mode. This criterion is a linear function where the argument in the x direction represents the effective normal stresses and in the y axis represents the shear stresses. Failure occurs by touching or exceeding this function. Another important feature of this criterion is the porepressure dependency. The effective normal stresses are the normal stresses reduced by the actual pore pressure. This can reduce the effective stress dramatically if the soil has a high water content.

The Rankin theory categorizes two different failure modes: the first one is the "active" failure, where horizontal strains lead to an expansion of the soil. The failure angles are $45° + \phi/2$. The second failure zone is the "passive" failure. It occurs by contracting the soil and leads to a failure angle of $45° - \phi/2$.

In debris flow, zones of active and passive earth pressure can change rapidly and therefore an accurate modeling of these pressures and their changes is of major importance.

Strain-dependent internal stresses

The stresses of debris flows have never been measured, but investigations of events and laboratory models have shown that there is a complex interaction between the internal strains and the stress distribution. Landslides do not spread out as fast as fluids, which can be explained by the Rankine´s earth pressure theory. Zones where the slide material begins to diverge should be described by the "active" stress, and where the material converge by the "passive stress". The 3D solution of this problem is far more complicated than the plain strain theory of Rankine. Therefore the internal stress distribution is approximated in a way that the stress and strain states fulfill the stress and strain symmetry rules and that they are independent from the chosen reference frame as far as possible.

2.1.3 Entrainment

Rapid landslides not only consist of their source material, but also of the entrained material. The entrained material consists mainly of deposits with a high water content. Rapid loading of those materials can lead to failure and mobilization of certain zones. This leads to volume changes and altering of the material, which can influence the impact area of such an event.

Mechanisms of entrainment

The mobilization of path material takes place at the margins and the base of a rapid landslide. On the margins mostly plowing occurs. The plowed material gets pushed downwards and may not necessarily be entrained in the main landslide mass. Plowing plays a major role where the slope angle decreases dramatically (McDougal, 2006). Another mechanism

is the bed material entrainment. It can occur when the basal shear stress gets exceeded, grain-bed interactions develop, or when liquefaction of the basal zones occurs.

Maximum erosion depth

There are two different approaches to evaluate the maximum erosion depth. The first approach aims at calculating the depth by assuming an unlimited bed ("supply unlimited") (Takahashi, 1978). These formulas include the flow depth, unit weight of water, the saturated weight of the bed material, bed inclination and the internal friction angle of the bed. Assuming drained or undrained loading leads to big differences in the results. Rapid landslides will probably lead to undrained loading, but due to the sensitivity of those equations to the drainage assumptions, a practicable usage of those equations is questionable (McDougal, 2006).

Another approach is the "supply limited" condition. Geological boundaries such as bedrock define the maximum erosion depth, which can be evaluated in the field.

Heterogeneities in the bed and bank failures are certainly important factors for the entrainment, but it is difficult to implement them in a dynamic model because the input is uncertain.

Momentum transfer

Entrainment leads to volume change during a debris flow event. These changes happen due to the momentum transfer of the moving mass onto the static bed material. The static bed material gets accelerated and transported downwards. Momentum gets conserved, but due to the inelastic collision, energy gets dissipated and velocity decreases. This leads to a reduced kinetic energy and shorter runouts. Therefore volume change leads to a velocity dependent resistance additional to the basal shear resistance.

2.1.4 Variations in rheology

Landslides such as debris flows have explicit material compositions. These compositions can influence the resistance and spreading of the sliding mass.

Variations along the path

Due to entrainment, the composition of the sliding mass can change. This leads to a different rheology of the material and therefore changes in the basal shear resistance. Also changes in the water ratio can influence the behavior of the debris flow, by changing the pore pressure. Another variation along the path can be the bed material on which the mass is sliding. When the bed becomes smoother, the runout will be longer and vice versa. Obstacles along the path (e.g. big boulders, trees) contribute another influence factor to the runout dynamics.

Variations within the landslide

Not only the rheology along the path can change, but also the rheology in the landslide itself. Landslides are transporting soil, rock and organic material (e.g. timber), whose composition, grain size, viscosity and pore pressure can change significantly over small domains (McDougal, 2006). Internal sorting can happen, which often leads to boulder fronts. This grain size segregation may influence the dynamics (McDougal, 2006). McDougal (2006) tried to implement internal rheology into the DAN3D code, but without any practical calculation approaches it was not possible.

2.2 Governing equations

2.2.1 Equivalent fluid

Rapid landslides are a complex dynamic phenomena that behave differently to normal hydraulic fluids. Standard hydrodynamic assumptions like hydrostatic and isotropic stresses and isotropic materials cannot be applied to materials consisting of a heterogeneous mixture of earth and water. Constitutive laws with simple physical relationships are difficult to apply and could be used only for controlled experiments (Denlinger and Iverson, 2001). Therefore Hungr (1995) defined a contrary semi - empirical approach based on the "equivalent fluid" concept. The heterogeneous soil and water mixture is modeled as a hypothetical homogeneous material with simple internal and basal rheology. The internal rheology is described by a frictional model, only using the internal friction angle ϕ_i. The

basal rheology can be described by several rheologies that consist of one or two parameters. These parameters do not derive from experimental or field measurements, but need to be evaluated by trial-and-error back-analysis of previous events.

2.2.2 Conservation laws

DAN3D uses a continuum approach which is only valid if the grain size is small in relation to the dimensions - especially the height of the landslide. This criterion may be violated in case of rockfalls consisting of some big boulders which exceed the mean slide height and concentrate stresses, or with clay flow slides where relatively large rafts of coherent material are transported. For fine grained debris flows, the laws of continuum mechanics are appropriate. If the debris flow contains bigger amounts of boulders, the results need to be viewed with skepticism and interpreted accordingly.

A derivation of the fundamental system of depth-averaged Lagrangian mass and moment balance equations used in DAN3D will be given in the following paragraphs. They describe the most important steps of their development, as well as the used assumptions and simplifications. All equations, assumptions and simplifications refer to the PhD thesis of McDougal (2006).

Initial equations

The Eulerian description of mass and momentum balance laws is the starting point for the derivation of the necessary equations. The first simplification is the definition of a spatial and temporal constant material density ($\partial\rho/\partial t = 0$, $\partial\rho/\partial x = 0$, $\partial\rho/\partial y = 0$ and $\partial\rho/\partial z = 0$). In general this means that the material is incompressible. Although spatial and temporal density variation occur in reality, these are mostly associated with dilation and contraction located in a thin layer near the base of the flowing material (Savage and Hutter, 1989). Density variations have been incorporated into dynamic models (Brufau et al., 2000) but did not improve the results, probably due to relatively small density variations compared to other dynamic variables (Denlinger and Iverson, 2004). Using this simplification produces the mass and momentum balance equations for a constant

material density. The first equation describes the mass balance:

$$\frac{\partial v_x}{\partial x} + \frac{\partial v_y}{\partial y} + \frac{\partial v_z}{\partial z} \tag{2.1}$$

The next three equations describe the momentum balance in the x, y and z direction respectively:

$$\rho\left(\frac{\partial v_x}{\partial t} + \frac{\partial (v_x^2)}{\partial x} + \frac{\partial (v_x v_y)}{\partial y} + \frac{\partial (v_x v_z)}{\partial z}\right) = -\left(\frac{\partial \sigma_x}{\partial x} + \frac{\partial \tau_{yx}}{\partial y} + \frac{\partial \tau_{zx}}{\partial z}\right) + \rho g_x \tag{2.2}$$

$$\rho\left(\frac{\partial v_y}{\partial t} + \frac{\partial (v_y v_x)}{\partial x} + \frac{\partial (v_y^2)}{\partial y} + \frac{\partial (v_y v_z)}{\partial z}\right) = -\left(\frac{\partial \tau_{xy}}{\partial x} + \frac{\partial \sigma_y}{\partial y} + \frac{\partial \tau_{zy}}{\partial z}\right) + \rho g_y \tag{2.3}$$

$$\rho\left(\frac{\partial v_z}{\partial t} + \frac{\partial (v_z v_x)}{\partial x} + \frac{\partial (v_z v_y)}{\partial y} + \frac{\partial (v_z^2)}{\partial z}\right) = -\left(\frac{\partial \tau_{xz}}{\partial x} + \frac{\partial \tau_{yz}}{\partial y} + \frac{\partial \sigma_z}{\partial z}\right) + \rho g_z \tag{2.4}$$

Where v is the velocity, σ is the normal stress, τ is the shear stress, ρ is the material density and g is the gravitational acceleration.

Applying boundary conditions

To solve these equations, kinematic and stress state boundary conditions at the surface ($z = b + h$) and bottom of the landslide ($z = b$) are introduced. For further calculations, b describes the height of the bed and h the height of the sliding mass. It is assumed that the surface of the sliding material is stress free. The stress condition at the bed is a combination of normal stresses due to the weight of the mass above and centripetal accelerations due to bed curvature. Another stress condition at the bottom of the sliding material are the basal shear stresses, which are described separately by the basal shear rheologies in section 2.2.3.

Again there are some assumptions to simplify the boundary conditions. First is is assumed that material does not enter or leave the landslide material at the free surface. With this assumption it is not possible to account for material that enters the sliding mass due to bank failures or possible ejection of the material bouncing out the surface. This leads to the first kinematic boundary condition for the surface of the sliding mass:

$$\frac{\partial(b+h)}{\partial t} + v_{x_{(z=b+h)}} \frac{\partial(b+h)}{\partial x} + v_{y_{(z=b+h)}} \frac{\partial(b+h)}{\partial y} - v_{z_{(z=b+h)}} = 0 \tag{2.5}$$

The next assumption is that there is only entrainment through the bed. Plowing in front of the landslide will be handled like bed entrainment, which is defined by E_t, the "erosion velocity" (Takahashi, 1991). Another assumption is that the bulk density of the entrained material is the same as the sliding material. This assumption can be justified in general. Often deposited material from previous slides lays in the path. In some cases the path material has a significantly different density (e.g. snow and ice) and therefore these assumptions are not valid. These two assumptions lead to the second kinematic boundary condition:

$$\frac{\partial b}{\partial t} + v_{x_{(z=h)}} \frac{\partial b}{\partial x} + v_{y_{(z=h)}} \frac{\partial b}{\partial y} - v_{z_{(z=h)}} = -E_t \tag{2.6}$$

Depth-averaging

In order to reduce the computational effort, the full 3D equations are translated to a quasi 3D form by integration between the bed and the free surface (like the classical St. Venant shallow water equations). Explicitly for the momentum balance, where $E_t \geq 0$, because deposition is included simply by removing its own share of momentum without influencing the momentum of the remaining sliding material. It is assumed that momentum correction due to differential advection does not need to be performed. Substitution of the kinematic boundary conditions into the balance equations and integrating them in the z direction leads to the most general form of the Eulerian, depth-averaged governing equations in the x, y and z direction respectively:

$$\begin{aligned} \rho \left[h \left(\frac{\partial \overline{v_x}}{\partial t} + \overline{v_x} \frac{\partial \overline{v_x}}{\partial x} + \overline{v_y} \frac{\partial \overline{v_y}}{\partial y} \right) + \left(\overline{v_x} - v_{x_{(z=b)}} \right) E_t \right] = \\ - \left[\frac{\partial(\overline{\sigma_x} h)}{\partial x} + \frac{\partial(\overline{\tau_{yx}} h)}{\partial y} + \left(\sigma_{x_{(z=b)}} \frac{\partial b}{\partial x} + \tau_{yx_{(z=b)}} \frac{\partial b}{\partial y} - \tau_{zx_{(z=b)}} \right) \right] + \rho h g_x \end{aligned} \tag{2.7}$$

$$\rho\left[h\left(\frac{\partial\overline{v_y}}{\partial t}+\overline{v_x}\frac{\partial\overline{v_y}}{\partial x}+\overline{v_y}\frac{\partial\overline{v_y}}{\partial y}\right)+\left(\overline{v_y}-v_{y_{(z=b)}}\right)E_t\right]= \\ -\left[\frac{\partial(\overline{\tau_{xy}}h)}{\partial x}+\frac{\partial(\overline{\sigma_y}h)}{\partial y}+\left(\tau_{xy_{(z=b)}}\frac{\partial b}{\partial x}+\sigma_{y_{(z=b)}}\frac{\partial b}{\partial y}-\tau_{zy_{(z=b)}}\right)\right]+\rho h g_y \quad (2.8)$$

$$\rho\left[h\left(\frac{\partial\overline{v_z}}{\partial t}+\overline{v_x}\frac{\partial\overline{v_z}}{\partial x}+\overline{v_y}\frac{\partial\overline{v_z}}{\partial y}\right)+\left(\overline{v_z}-v_{z_{(z=b)}}\right)E_t\right]= \\ -\left[\frac{\partial(\overline{\tau_{xz}}h)}{\partial x}+\frac{\partial(\overline{\tau_{yz}}h)}{\partial y}+\left(\tau_{xz_{(z=b)}}\frac{\partial b}{\partial x}+\tau_{yz_{(z=b)}}\frac{\partial b}{\partial y}-\sigma_{z_{(z=b)}}\right)\right]+\rho h g_z \quad (2.9)$$

Lagrangian reference frame

DAN3D works with a Lagrangian reference frame. Therefore, the previous established equations written in the Eulerian reference frame need to be transformed. During this process additional simplifications were made:

- Classical shallow flow assumptions, where the shear stress derivatives of τ_{xz} and τ_{yz} can be neglected. This simplification is argued by the fact that depth variations are gradually and relatively small in comparison to the length and width of a landslide.
- The Lagrangian derivative of v_z is set to the centripetal acceleration due to the bed-normal curvature in direction of motion.
- The calculation of the total bed-normal stress at the base includes the weight of the material above and the centripetal acceleration. If there is a negative vertical acceleration, the mass becomes airborne. In reality, the impact after free fall leads to energy losses. DAN3D does not account for those energy losses yet. It needs to be included somehow in the basal shear strength term.
- Using the Rankine earth pressure theory, σ_x and σ_y can be described as $\sigma_x = k_x\sigma_z$ and $\sigma_y = k_y\sigma_z$. Also spatial variation of the pressure coefficient k_i are neglected, because it is assumed that they are relatively small.

Collecting terms and transforming them to the Lagrangian form, the depth-averaged mass balance takes the following form:

$$\frac{dh}{dt} + h\left(\frac{\partial \overline{v_x}}{\partial x} + \frac{\partial \overline{v_y}}{\partial y}\right) = E_x \tag{2.10}$$

Using these simplifications, several mathematical operations and substituting the mass balance into equation (2.10), the final Lagrangian form of the depth-averaged momentum balance equations can be written in the x and y direction:

$$\rho h \frac{D\overline{v_x}}{Dt} = \rho h g_x - k_x \sigma_{z_{(z=b)}} \frac{\partial h}{\partial x} - k_{yx} \sigma_{z_{(z=b)}} \frac{\partial h}{\partial y} + \tau_{zx_{(z=h)}} - \rho\left(\overline{v_x} - v_{x_{(z=b)}}\right) E_t \tag{2.11}$$

$$\rho h \frac{D\overline{v_y}}{Dt} = \rho h g_y - k_y \sigma_{z_{(z=b)}} \frac{\partial h}{\partial y} - k_{xy} \sigma_{z_{(z=b)}} \frac{\partial h}{\partial x} \tag{2.12}$$

2.2.3 Basal shear resistance

DAN 3D allows the user to choose between six different rheologies: laminar, turbulent, plastic, Bingham, frictional and Voellmy. This master thesis focuses on the frictional and Voellmy rheology because those are most commonly used in current research. The basal shear resistance controls the runout process and has a big overall importance for the model behavior. Choosing a proper rheology with its resistance parameters has a comparable importance to a correct 3D terrain. The following equations are from McDougal (2006).

Voellmy

The so called Voellmy rheology is a combination of a frictional resistance term and a turbulence term:

$$\tau_{zx_{(z=h)}} = -\left(\sigma_{z_{(z=h)}} f + \frac{\rho g \bar{v}_x^2}{\xi}\right) \tag{2.13}$$

where $\tau_{zx_{(z=h)}}$ $[\frac{\mathrm{N}}{\mathrm{m}^2}]$ is the basal shear stress, $\sigma_{z_{(z=h)}}$ $[\frac{\mathrm{N}}{\mathrm{m}^2}]$ is the bed-normal stress, f [-] is the dimensionless friction coefficient, ρ $[\frac{\mathrm{kg}}{\mathrm{m}^3}]$ is the density, g $[\frac{\mathrm{m}}{\mathrm{s}^2}]$ is the gravitational acceleration, $\bar{v}_x^2$ $[\frac{\mathrm{m}^2}{\mathrm{s}^2}]$ is the square of the mean velocity, and ξ $[\frac{\mathrm{m}}{\mathrm{s}^2}]$ is the so called turbulence parameter.

The first term of equation 2.13 describes the normal stress dependent flow resistance.

Landslides, especially debris flows occur mainly on saturated slopes. The pore pressure reduces by decreasing the effective stresses the adhesion forces on the sliding slip, which are responsible for the friction resistance. The non-dimensional coefficient f describes a friction coefficient which is dependent by the dynamic friction angle ϕ, the pore pressure ratio r_u (McLellan and Kaiser, 1984) and the normal stress σ_z.

$$f = \tan \phi_b = (1 - r_u) \tan \phi \tag{2.14}$$

$$r_u = \frac{u}{\sigma_z} \tag{2.15}$$

The second term of equation 2.13, the so called turbulence therm, was developed by Voellmy (1955) for the calculation of snow avalanche dynamics. Voellmy used this equation for the incorporation of a velocity dependent turbulent resistance. This relationship came from the hydraulics where ξ describes the square of the Chézy coefficient C. The physical explanation for the turbulent resistance in rapid landslides are local velocity fluctuations and viscous forces of particles, which lead to a transfer in momentum (Chen and Lee, 2003a).

Frictional

The frictional rheology depends on the pore pressure ratio r_u, the basal friction angle ϕ and the effective stress σ. Granular materials often have a frictional behavior (McDougal, 2006). In order to get reliable results using this basal rheology, the pore pressure ratio r_u and the friction angle ϕ need to be estimated. The bulk friction angle ϕ_b which includes the pore pressure coefficient r_u can be calculated with equation 2.16. In literature most authors state ϕ_b. The input of DAN3D needs the basal friction angle ϕ which can be evaluated with equation 2.17. The basal shear resistance at the transition zone between the sliding material and the surface can be calculated using equation 2.18

$$\phi_b = \arctan (1 - r_u) \tan \phi \tag{2.16}$$

$$\phi = \arctan \frac{\phi_b}{\arctan\left(1 - r_u\right)} \tag{2.17}$$

$$\tau_{zx_{(z=b)}} = -\sigma_{z_{z=b}} \tan \phi_b \tag{2.18}$$

The following four rheologies are not used in this thesis and are therefore only mentioned in order to indicate the full possibilities of DAN3D.

Laminar

$$\tau_{zx_{(z=b)}} = -\frac{3\mu\overline{v_x}}{h} \tag{2.19}$$

Where μ is the dynamic viscosity, $\overline{v_x}$ the depth averaged flow velocity in the main direction, and h the flow depth.

Turbulent

$$\tau_{zx_{(z=b)}} = -\frac{\rho g n^2 \overline{v_x}^2}{h^{1/3}} \tag{2.20}$$

Where ρ is the material density, n the Manning roughness coefficient, $\overline{v_x}$ the depth averaged flow velocity and h the flow depth.

Plastic

$$\tau_{zx_{(z=b)}} = -c \tag{2.21}$$

Where c is a constant shear strength parameter.

Bingham

$$\tau^3_{zx_{(z=b)}} + 3\left(\frac{\tau_{yield}}{2} + \frac{\mu_{Bingham}\overline{v_x}}{h}\right)\tau^2_{zx_{(z=b)}} - \frac{\tau^3_{yield}}{2} = 0 \tag{2.22}$$

The cubic equation 2.22 needs to be solved to estimate the basal shear resistance, where τ_{yield} is the Bingham yield stress and $\mu_{Bingham}$ the Bingham viscosity.

2.2.4 Numerical solution

The numerical solution of the balance equations is solved using the Smoothed Particle Hydrodynamics method. This method is mesh-less and describes the continuum of the landslide mass with particles that are influencing each other. Calculations are performed directly at the locations of the particle. Depending to the vicinity of the particles the influence increases, and on the other hand if a certain trashold distance is exceeded there is no influence.

To simplify the calculation procedure, the incremental transverse shear strain $\delta\gamma_{xy}$ is set to zero. This leads to $\tau_{xy} = 0$ and $\tau_{xy} = 0$. With this assumption, the governing equation of momentum balance changes to the following (McDougal, 2006):

$$\rho h \frac{D\overline{v_x}}{Dt} = \rho h g_x - k_x \sigma_{z_{(z=b)}} \frac{\partial h}{\partial x} + \tau_{zx_{(z=h)}} - \rho \left(\overline{v_x} - v_{x_{(z=b)}} \right) E_t \tag{2.23}$$

$$\rho h \frac{D\overline{v_y}}{Dt} = \rho h g_y - k_y \sigma_{z_{(z=b)}} \frac{\partial h}{\partial y} \tag{2.24}$$

Further simplifications are the decoupling of the x and y direction (which means that the Poisson ratio is zero) and the setting of a constant default normalized elastic stiffness modulus of $D = E\sigma_z = 200$. Model investigations about the influence of D showed that DAN3D is not very sensitive to it (McDougal, 2006).

The "entrainment ratio" E_t is replaced by the empirical displacement-dependent erosion rate E_s. It is a constant (it can be defined on each grid cell by the user) entrainment value which describes the amount of entrained volume per meter traveled depending on the local flow. Using equation 2.25, E_s can be substituted by the governing equations. There is no velocity dependency in the erosion rate E_s, or any other factor which can influence the erosion rate. Therefore different erosion rates on certain grid locations can account for those effects to create a pseudo dependent erosion rate.

$$E_t = E_s h \overline{v_x} \tag{2.25}$$

Finally the particle values can be transformed to grid cell based values with a direct plot in the program. The grid cell based values create contour maps of velocity, heigth,

maximum velocity and maximum height. Using these graphical results, hazard mapping can be performed. For more details it is referred to the PhD. thesis of McDougal (2006).

2.3 Basal friction resistance used in other debris flow capable models

Different basal friction resistance approaches are used in other rapid landslide models. The following paragraphs are a brief list of different models and their rheologies used along the 2007 International Forum on Landslide Disaster Management (Ho and Li, 2007).

FLO-2D

FLO-2D (O´Brien, 1993) uses depth-averaged equations which describe the conservation of mass and momentum flow. This model was used to back-analyze the 2005 Tate´s Cairn Debris Flow (Hong Kong), where an estimated volume of about 2500 m^3 were triggered from an initial source volume of approximately 1000 m^3 (Cepeda, 2008). Equation 2.26 shows the basal resistance term used in FLO-2D

$$\tau = \tau_y + \frac{K\eta\nu}{8h} + \frac{\gamma {n_{td}}^2 \nu^2}{h^{1/3}} \tag{2.26}$$

where τ is the basal shear stress, τ_y is the yield stress, K is a dimensionless resistance parameter which increases with roughness and irregularity of the cross section geometry, η is the flow viscosity, h is the flow depth and n_{td} is a modified Manning´s n value. The yield stress τ_y and viscosity ν are dependent on the sediment concentration and can be calculated with regression constants provided by the software.

For this event FLO-2D could not match both the deposit position and debris flow velocity. The simulation which best fits the runout and underestimates the velocity uses the following parameters: sediment concentration = constant and 0.37, $n = 0.04$, $\tau_y = 240$ Pa, $\eta = 13$ Pas. The best fitting results with DAN3D are obtained with the following parameters: $\phi = 15°$, $\xi = 1000$ m/s^2.

Wang

This model has been developed at the University of Alberta by Wang (2008). It satisfies the equation of motion, the continuity equation, the energy equation and the constitutive description of the material. The basal resistance term is described by the Mohr Coulomb friction.

2.27

$$\tau = c + \sigma \tan \phi_b \tag{2.27}$$

where c is the cohesion, σ is the normal stress and ϕ_b is the basal friction angle.

Chan et al. (2008) investigated four debris flow events which used the following model parameters:

- Lo Wai Debris Flood (2005) - $\gamma = 20$ kN/m^3, $\phi_i = 30°$ and $\phi_b = 9°$
- Sham Tseng San Tsuen Debris Flow - $\gamma = 20$ kN/m^3, $\phi_i = 35°$ and $\phi_b = 20°$
- Tsing Shan Debris Flow (1990) - $\gamma = 20$ kN/m^3, $\phi_i = 35°$ and $\phi_b = 24°$
- Tsing Shan Debris Flow (2000) - $\gamma = 20$ kN/m^3, $\phi_i = 30°$ and $\phi_b = 14°$

FLATModel

The FLATModel (Median et al., 2008) is a 2D-finite volume model created in collaboration with the hydraulic and geotechnical departments of the Technical University of Catalonia (Barcelona, Spain). The basal resistance term 2.28 equals the Mohr Coulomb rheology.

$$\tau = c + h\rho g \cos \Phi \tan \phi_{bed} \tag{2.28}$$

where c is the cohesion, h is the debris height, ρ is the the material density, g the gravitational acceleration, Φ is the channel bed inclination, ϕ_{bed} is the basal friction angle and σ is the normal stress.

Hürlimann et al. (2008) investigated two debris flow events which used the following model parameters:

- Tsing Shan Debris Flow (1990) - $\phi = 11.3°$, $C_z = 8$ m$^{1/2}$ and $\phi_{bed} = 37°$

- Tsing Shan Debris Flow (2000) - $\phi = 8.53°$ and $C_z = 20$ m$^{1/2}$

3d Debris Mobility Model (3dDMM)

3dDMM was developed by the Geotechnical Engineering Office (GEO) of the Hong Kong Government to simulate 3D landslide runouts. It is a continuum model where the momentum equations are solved and Voellmy 2.29 and frictional rheologies are implemented (Kwan and Sun, 2008).

$$\tau_{zx} = \frac{-u}{\sqrt{u^2 + v^2}} \left[\sigma_z \tan\delta + \rho g \frac{u^2 + v^2}{\xi} \right] \tag{2.29}$$

$$\tau_{zy} = \frac{-v}{\sqrt{u^2 + v^2}} \left[\sigma_z \tan\delta + \rho g \frac{u^2 + v^2}{\xi} \right] \tag{2.30}$$

where u and v are the depth-averaged debris velocities in the x and y directions respectively, σ_z is the normal stress at the debris base, δ is the dynamic friction angle at the debris base, ρ is the debris bulk density, g is the gravitational acceleration and ξ is the Voellmy coefficient.

Kwan and Sun (2008) investigated three debris flow events which used model parameters are the following:

- Sham Tseng San Tsuen Debris Flow - $\delta = 12°$ and $\xi = 500$m/s^2
- Tsing Shan Debris Flow (1990) - $\delta = 15°$ and $\xi = 500$m/s^2
- Tsing Shan Debris Flow (2000) - $\delta = 15°$ and $\xi = 500$m/s^2

RASH3D

RASH3D is a single-phase continuum mechanics code developed by Pirulli (2005) and implements four different rheologies (Pirulli and Scavia, 2008):

1. Frictional rheology

$$\tau_{zi(i=x,y)} = -\left(\gamma \cos\alpha h \tan\delta\right) \frac{v_i}{\|v\|} \tag{2.31}$$

where τ_{zi} are shear resistance stresses, γ is the unit weight, h is the flow depth, δ is the constant friction angle and v_i are velocities.

2. Voellmy rheology

$$\tau_{zi(i=x,y)} = -\left(\gamma \cos\alpha h \tan\delta' + \frac{\gamma \overline{v_i}^2}{\xi}\right)\frac{v_i}{\|v\|} \tag{2.32}$$

where $\overline{v}$ is the mean flow velocity, ξ is the turbulence coefficient and the other terms are similar to equation 2.31

3. Quadratic rheology

$$\tau_{zi(i=x,y)} = -\left(\tau_y + \frac{\gamma {n_{td}}^2 \overline{v_i}^2}{h^{1/3}}\right)\frac{v_i}{\|v\|} - \frac{k\eta\overline{v_i}}{8h} \tag{2.33}$$

where τ_y is the Bingham yield stress, η is the Bingham viscosity, n_{td} is the equivalent Manning´s coefficient and k is the flow resistance parameter.

4. Empiric frictional

$$\mu = \tan\delta_1 + (\tan\delta_2 - \tan\delta_1)\exp\left(-\beta\frac{h}{dL}\frac{\sqrt{gh}}{v}\right) \tag{2.34}$$

where μ is a empirical friction coefficient, δ_1 and δ_2 are the range of the friction angle depending on the velocity and thickness of the flow, β is a material dependent constant function, d is the mean particle diameter and L is a constant assumed to be 10.

Pirulli and Scavia (2008) investigated the Tates´ Cairn Debris Flow (Hong Kong 2005). The applied basal friction rheologies and their best-fit model parameters are the following:

- Frictional: $\delta = 27°$
- Voellmy: $\delta' = 25°$ and $\xi = 1000$ m/s^2
- Quadratic: $\tau_y = 1.2$ kPa, $\eta = 40$ Pas and $n = 0.03$

Chapter 3

Inputs for DAN3D

3.1 Introduction

DAN3D requires data of the examined area to be able to run a computation. Using several different software made it possible to create the needed files in a proper and efficient way. In general either a back-analysis or a prediction were performed. Therefore different data are available, that needs to be reconditioned or estimated from scratch.

DAN3D needs 3 grid files as input for the computation. These are grids for the path topology, the source and the entrainment.

The following sections describe the general steps to get the needed Surfer grid files.

3.2 Specifications of the 3 DAN3D grid files

All three grid files need to have the same number of grids in each direction with the same grid size. The program is limited to a size of 400 rows and 400 columns. The *.GRD file is written in ASCII code which can be generated using the software SURFER.

The following specifications are given by the interim instructions of DAN3D (Hungr, 2006).

- The source grid file describes the difference of the source area before and after the landslide. The grid needs to be zero in the deposition area and is nowhere allowed to be negative.

- The path surface grid file describes the slide surface of the debris flow. It can be created by using the surface grid before the landslide subtracting the source grid of the debris flow.

- The erosion thickness grid file describes areas with their maximum entrainment depths. Entrainment will occur only where the grid is overrun by the landslide. Therefore the area can be bigger than the predicted erosion zone without harming the simulation. Where is no entrainment, the grid needs to be zero.

3.3 Creating a grid file

The creation of the grid files can be separated in two steps. First general grids need to be created. A valuable software for this purpose is ArcMap2010. It can generate grid files from several input data and save it in the Esri grid format which can be read by SURFER. When grid data is available in ASCII code, SURFER can already handle it without any preprocessing.

Secondly the Esri grid can be transformed into the .GRD format using the software SURFER. ASCII grid data needs to be gridded by SURFER and therefore a proper gridding algorithm, grid spacing and grid extent need to be specified.

The preprocessing of the grid files depends on the purpose of the model and is therefore described separately in chapter 5.

Chapter 4

Sensibility analyses

DAN3D is a calibration-based model. Therefore the understanding of the model parameters is of highest importance in order to get reliable results. Excluding the model options parameters (e.g. velocity smoothing coefficient), six parameters need to be defined. Performing a best fit back calculation of an event can yield the applied criterion using non realistic parameters. It is unclear how much influence those parameters have on certain results, if there are direct relationships, and if yes in which magnitude. A simplified model was created on which a sensibility analysis was performed.

4.1 Model geometry

A simplified path, source and erosion grid file needed to be created. The idea behind the simplification of the grid files was to get more comparable results by avoiding geometrical based stress concentrations and such. The path grid is a combination of a steep valley with a length of 1455 m and an inclination of 1:1.63 and a runout area with a length of 753m and an inclination of 1:10. These values represent a realistic simplification of an alpine mountain valley prone to debris flow (figure 4.1, figure 4.2 and figure 4.3).

4.2 Model parameters for the sensibility analysis

Excluding the model option parameters, DAN3D has 8 variables. The control parameters need to be set at the start of the program and are the following: number of materials,

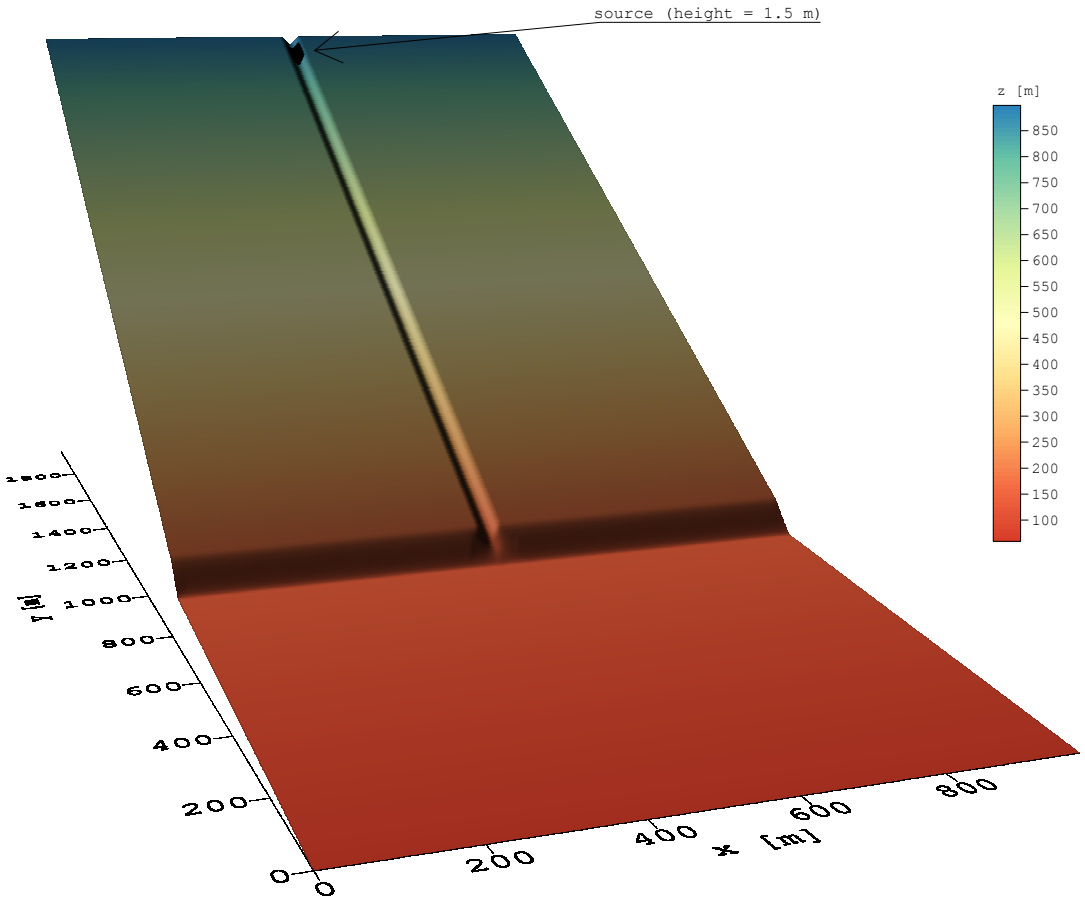

Figure 4.1 – Perspective view on the model (path and source)

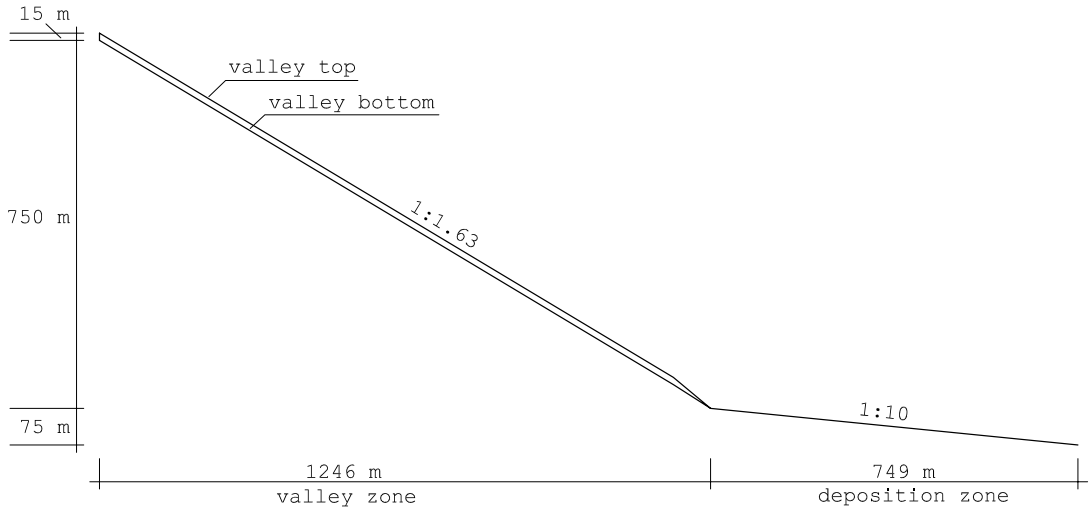

Figure 4.2 – Longitudinal section of the model

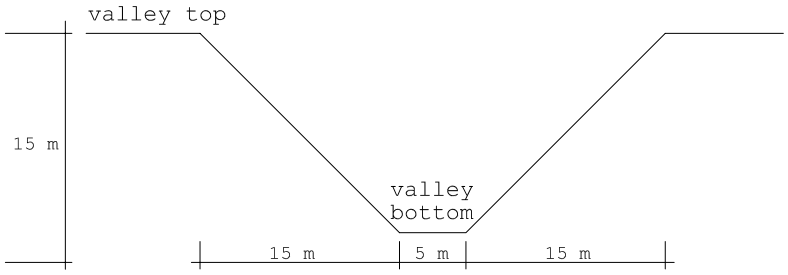

Figure 4.3 – Cross-section of the valley

number of particles, erosion rate E_s and time step. The other variables can be set in the material properties dialog and are dependent on the chosen rheology.

This parametric study only uses the Voellmy rheology and therefore the unit weight γ, friction coefficient f, turbulence coefficient ξ and internal friction angle ϕ needed to be specified. Additional to those parameters also the input grid files can be defined as variables. For this sensitivity analysis the influence of the initial volume V and the erosion rate E_s on the model behavior were studied.

For every model the number of particles was set to the maximum of 4000 particles, because it is obvious that more particles lead to better results (it is assumed that the computational algorithm works correctly). The number of materials was always set to 1. Adding more materials would complicate the analysis. The time-step is a constant in the following computations and is set to 0.1 s (which delivered good computational results).

Therefore 6 variables and their central values were defined and summarized in table 4.1. For every parameter 9-11 computations were performed, using a bandwidth of values spreading around the central value. It is important that every study has just one variable parameter and the other 5 parameters stay constant using the defined central value.

Table 4.1 – Central parameter values for the sensibility analysis

	$\gamma[kN/m^3]$	$f[-]$	$\xi[m/s^2]$	$\phi_i[°]$	$E_s[m^3/m]$	$V[m^3]$
C	*18*	*0.12*	*500*	*18*	*0.00064*	*2250*

Tables 4.2 ÷ 4.7 show the used parameters for every parameter study, which are labeled from a ÷ f.

Table 4.2 – Input parameters, variation of the unit weight $\gamma[kN/m^3]$

	$\gamma[kN/m^3]$	$f[-]$	$\xi[m/s^2]$	$\phi_i[°]$	$E_s[m^3/m]$	$V[m^3]$
a 01	**13**	0.12	500	18	0.00064	2250
a 02	**14**	0.12	500	18	0.00064	2250
a 03	**15**	0.12	500	18	0.00064	2250
a 04	**16**	0.12	500	18	0.00064	2250
a 05	**17**	0.12	500	18	0.00064	2250
a 06	*18*	*0.12*	*500*	*18*	*0.00064*	*2250*
a 07	**19**	0.12	500	18	0.00064	2250
a 08	**20**	0.12	500	18	0.00064	2250
a 09	**21**	0.12	500	18	0.00064	2250
a 10	**22**	0.12	500	18	0.00064	2250
a 11	**23**	0.12	500	18	0.00064	2250

Table 4.3 – Input parameters, variation of the friction coefficient $f[-]$

	$\gamma[kN/m^3]$	$f[-]$	$\xi[m/s^2]$	$\phi_i[°]$	$E_s[m^3/m]$	$V[m^3]$
b 01	18	**0.08**	500	18	0.00064	2250
b 02	18	**0.09**	500	18	0.00064	2250
b 03	18	**0.10**	500	18	0.00064	2250
b 04	18	**0.11**	500	18	0.00064	2250
b 05	*18*	*0.12*	*500*	*18*	*0.00064*	*2250*
b 06	18	**0.13**	500	18	0.00064	2250
b 07	18	**0.14**	500	18	0.00064	2250
b 08	18	**0.15**	500	18	0.00064	2250
b 09	18	**0.16**	500	18	0.00064	2250

Table 4.4 – Input parameters, variation of the turbulence coefficient $\xi[-]$

	$\gamma[kN/m^3]$	$f[-]$	$\xi[m/s^2]$	$\phi_i[°]$	$E_s[m^3/m]$	$V[m^3]$
c 01	18	0.12	**100**	18	0.00064	2250
c 02	18	0.12	**200**	18	0.00064	2250
c 03	18	0.12	**300**	18	0.00064	2250
c 04	18	0.12	**400**	18	0.00064	2250
c 05	*18*	*0.12*	*500*	*18*	*0.00064*	*2250*
c 06	18	0.12	**600**	18	0.00064	2250
c 07	18	0.12	**700**	18	0.00064	2250
c 08	18	0.12	**800**	18	0.00064	2250
c 09	18	0.12	**900**	18	0.00064	2250
c 10	18	0.12	**1000**	18	0.00064	2250

Table 4.5 – Input parameters, variation of the internal friction angle $\phi_i[°]$

	$\gamma[kN/m^3]$	$f[-]$	$\xi[m/s^2]$	$\phi_i[°]$	$E_s[m^3/m]$	$V[m^3]$
d 01	18	0.12	500	**10**	0.00064	2250
d 02	18	0.12	500	**12**	0.00064	2250
d 03	18	0.12	500	**14**	0.00064	2250
d 04	18	0.12	500	**16**	0.00064	2250
d 05	*18*	*0.12*	*500*	*18*	*0.00064*	*2250*
d 06	18	0.12	500	**20**	0.00064	2250
d 07	18	0.12	500	**22**	0.00064	2250
d 08	18	0.12	500	**24**	0.00064	2250
d 09	18	0.12	500	**26**	0.00064	2250
d 10	18	0.12	500	**28**	0.00064	2250
d 11	18	0.12	500	**30**	0.00064	2250

Table 4.6 – Input parameters, variation of the erosion rate $E_s[m^3/m]$

	$\gamma[kN/m^3]$	$f[-]$	$\xi[m/s^2]$	$\phi_i[°]$	$E_s[m^3/m]$	$V[m^3]$
e 01	18	0.12	500	18	**0.00000**	2250
e 02	18	0.12	500	18	**0.00015**	2250
e 03	18	0.12	500	18	**0.00027**	2250
e 04	18	0.12	500	18	**0.00038**	2250
e 05	18	0.12	500	18	**0.00047**	2250
e 06	18	0.12	500	18	**0.00055**	2250
e 07	*18*	*0.12*	*500*	*18*	*0.00064*	*2250*
e 08	18	0.12	500	18	**0.00088**	2250
e 09	18	0.12	500	18	**0.00111**	2250
e 10	18	0.12	500	18	**0.00184**	2250
e 11	18	0.12	500	18	**0.00368**	2250

Table 4.7 – Input parameters, variation of the source volume $V[m^3]$

	$\gamma[kN/m^3]$	$f[-]$	$\xi[m/s^2]$	$\phi_i[°]$	$E_s[m^3/m]$	$V[m^3]$
f 01	18	0.12	500	18	0.00064	**750**
f 02	18	0.12	500	18	0.00064	**1125**
f 03	18	0.12	500	18	0.00064	**1500**
f 04	18	0.12	500	18	0.00064	**1875**
f 05	*18*	*0.12*	*500*	*18*	*0.00064*	*2250*
f 06	18	0.12	500	18	0.00064	**2625**
f 07	18	0.12	500	18	0.00064	**3000**
f 08	18	0.12	500	18	0.00064	**3375**
f 09	18	0.12	500	18	0.00064	**3750**
f 10	18	0.12	500	18	0.00064	**4125**
f 11	18	0.12	500	18	0.00064	**4500**

4.3 Computation & data reconditioning

To get comparable results, the computations needed to be carried out in a standardized manner. First step was to define the results which sensibility should be analyzed. For the practical usage of a debris flow modeling program, the most important results are the maximum height, runout length, deposit area, deposit volume and the maximum and mean velocity. A simulation time of 240 s was defined to get comparable results. Some models showed minor movement after this time-step, which can be neglected because there are only some particles in movement thatdo not influence the results. The deposit area and deposit volume includes only the debris material which reached the runout slope. Some material was still in movement in the valley, but that does not affect the results because of their small magnitude. The velocities were analyzed in the part of the valley and do not include the deposition time.

The output of contour plots for every timestep, a ASCII grid file of the deposit (t = 240 s) and the maximum velocity could be automated using the program Scripter (from Surfer 9). These results were analyzed using ArcMap and Matlab. To get comparable values, the results and used parameter needed to be normalized by their central values.

4.4 Results of the sensibility analysis

The following graphs show the normalized results, their linear connection with a line and a linear regression line to get an idea about their dependency on the input parameter.

4.4.1 Variation of the unit weight γ

The variation of the unit weight showed no direct correlation to the results. Though two interesting differences in the results were found.

- The maximum velocity and the maximum height showed bigger spreading. The maximum velocity spreaded between 0 and 14.8 % and the maximum height between -16.9 and 4.3 %. But no correlation between the parameter variation and the maximum velocity and maximum height were found.

- The other results (e.g runout length) showed almost no dependency on the variation of the unit weight. The runout length and deposition area showed some minor spreading in contrast to the deposit volume and mean velocity where the spreading was in the order of one percent.

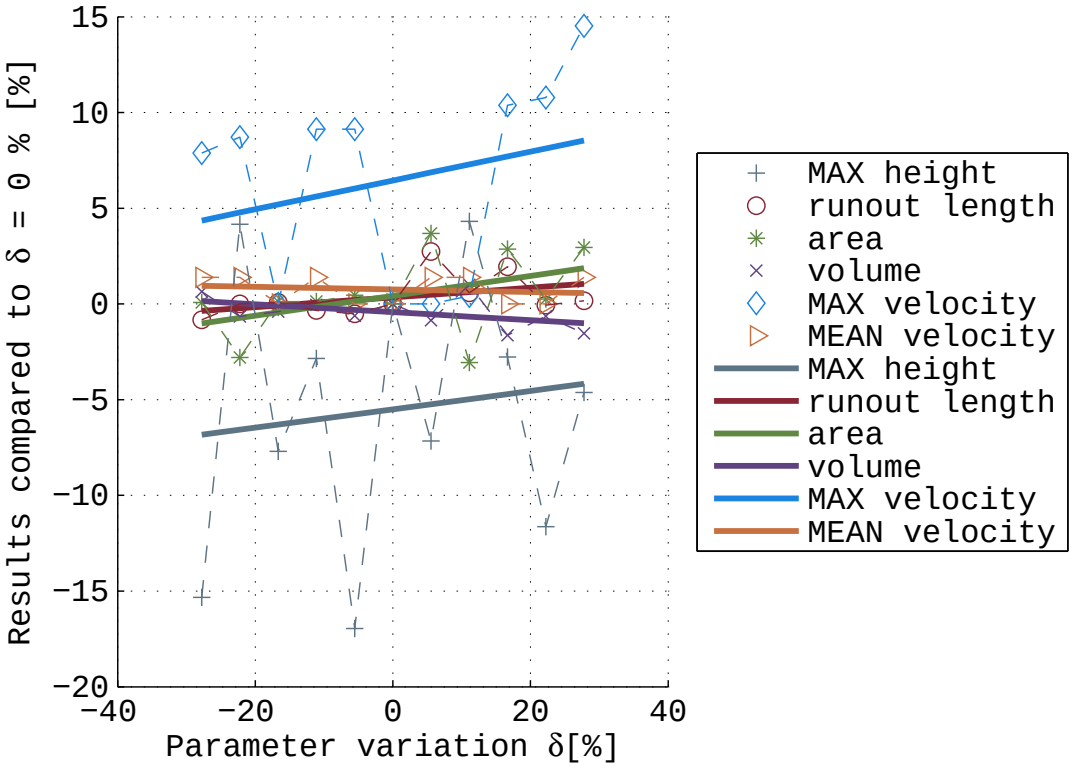

Figure 4.4 – Variation of the unit weight from 13 - 23 kN/m^3

4.4.2 Variation of the friction coefficient f

The friction coefficient had great influence on the results. Only the max velocity and the mean velocity were almost independent. The runout length and deposit area were influenced in the same way by the friction coefficient. They showed an exponential decrease with an increasing friction coefficient. The max height and the deposit volume were more or less positive linear dependent on the friction coefficient, where the height was about two times more sensible then the deposit volume.

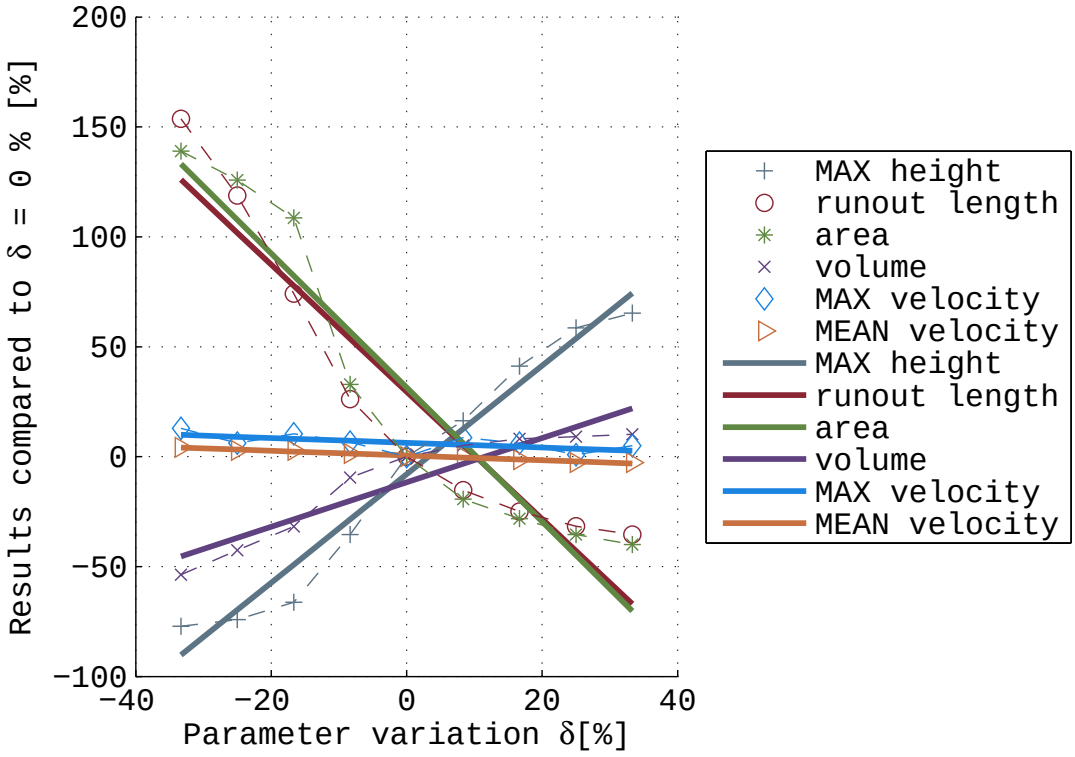

Figure 4.5 – Variation of the friction coefficient from 0.08 - 0.16

4.4.3 Variation of the turbulence coefficient ξ

This variation showed almost opposite dependencies compared to the friction coefficient. This can be explained by the formula of the shear resistance (2.13). The turbulence term is in the denominator and therefore decreases the frictional resistance. The frictional coefficient is in the numerator and therefore increases the frictional resistance. With a higher turbulence coefficient the debris mass could flow further and spread over a bigger area. Also the max and mean velocity showed the same sensibility. Only the volume and max height showed different dependencies. The max height decreased exponentially when increasing the turbulence coefficient. On the other hand, increasing the turbulence coefficient resulted in a decrease of the deposit volume.

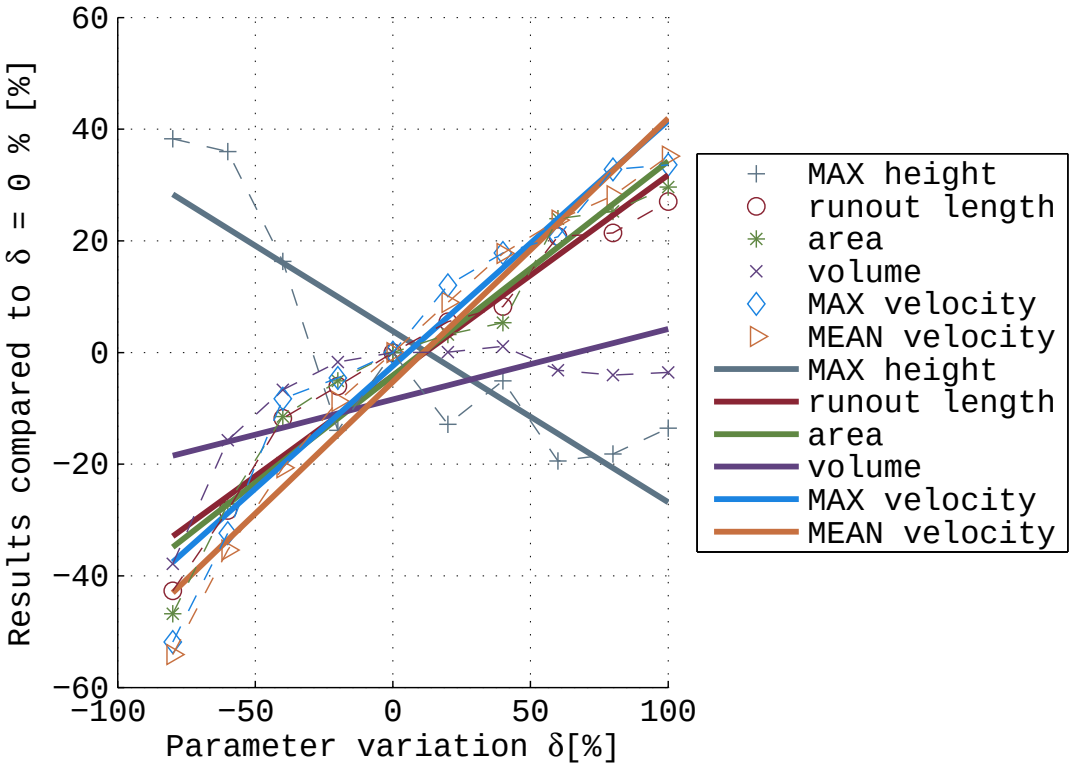

Figure 4.6 – Variation of the turbulence coefficient from 100 - 1000 m/s^2

4.4.4 Variation of the internal friction angle ϕ_i

The results of this sensibility analysis showed a negative dependency of the max height. This means that increasing the internal friction angle leads to a flatter deposit. Also the volume and the mean velocity were negatively dependent on the internal friction angle. On the other hand, the deposit area and the runout length were positively correlated. Only the max velocity did not show a clear correlation.

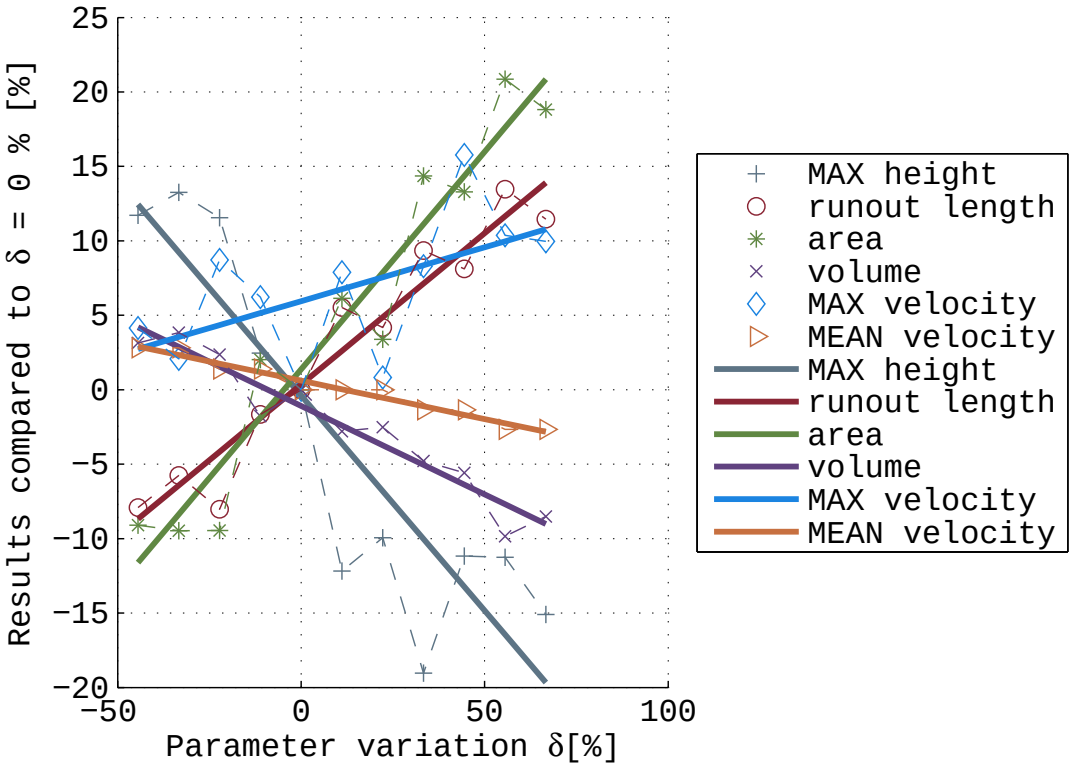

Figure 4.7 – Variation of the internal friction angle from 10° - 30°

4.4.5 Variation of the erosion rate E_s

The volume and deposit area were exponentially positive correlated with the erosion rate. This could be explained by the exponential influence on the entrainment volume by the erosion rate. The other results were linearly positive correlated with the erosion rate.

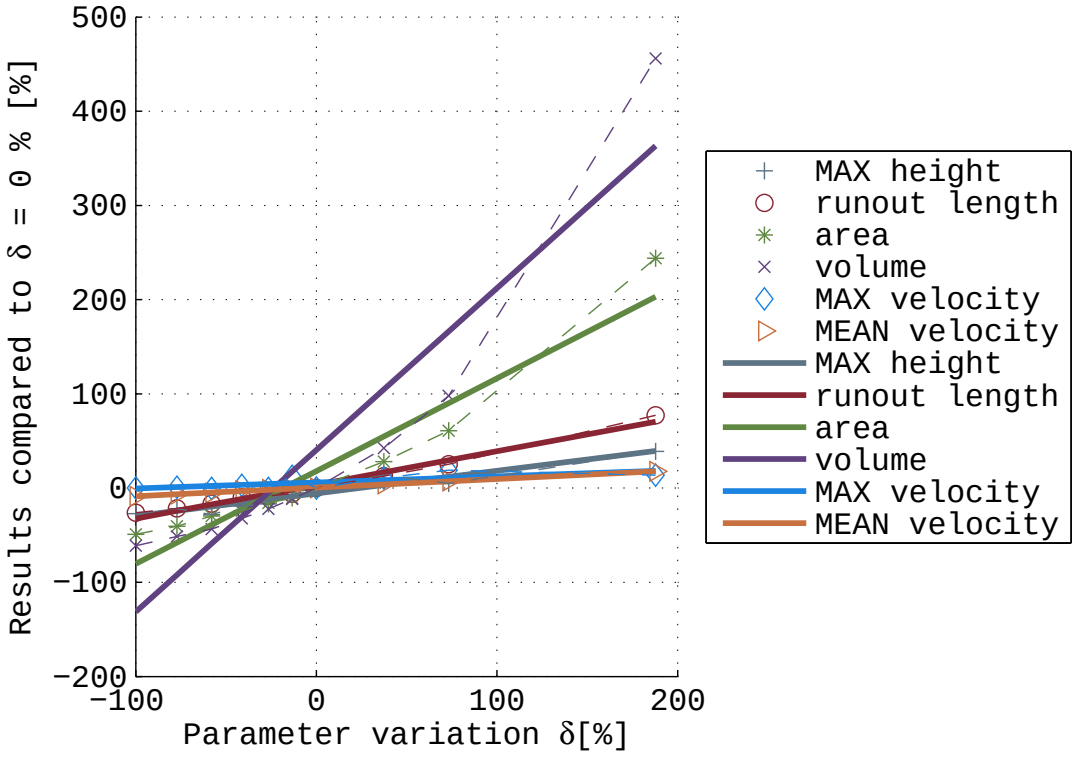

Figure 4.8 – Variation of the erosion rate from 0 - 0.00184 m^3/m

4.4.6 Variation of the source volume V

Variating the source volume leaded to a positive linear correlation on all observed results. The volume and deposit area were the most sensitive ones. The other parameters were correlated positive linear, but in a smaller magnitude compared to the deposit volume and deposit area.

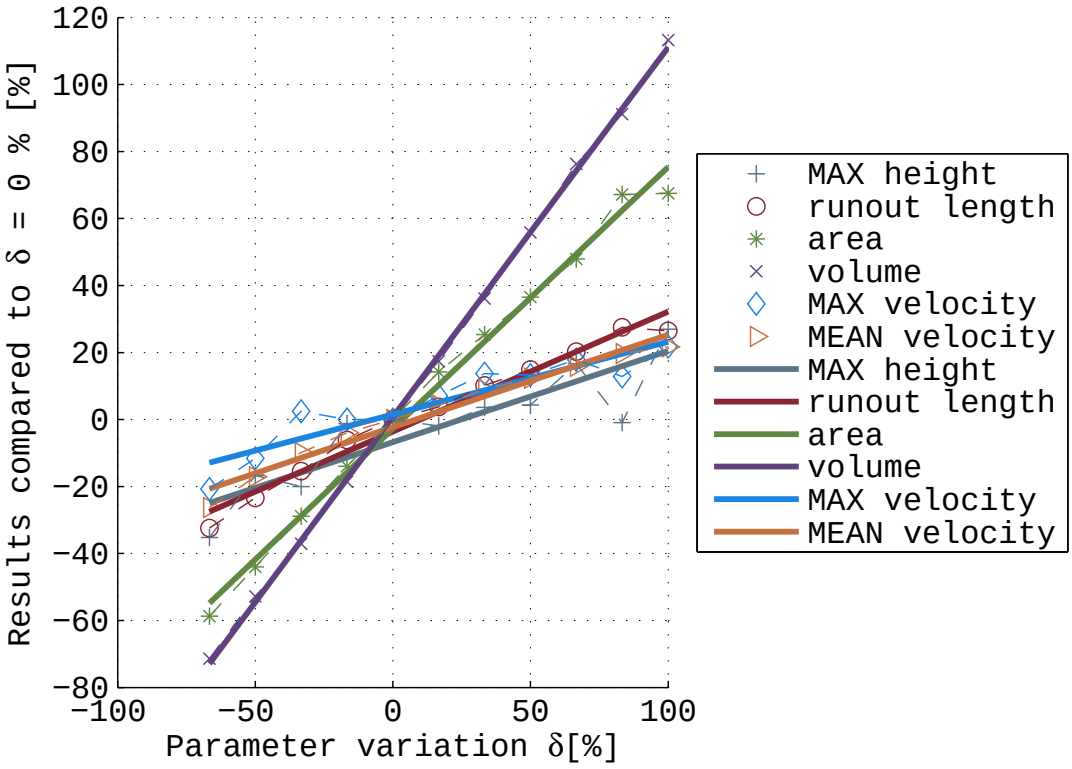

Figure 4.9 – Variation of the source volume from 750 - 4500 m^3

4.4.7 Sensibility shown by the gradient of the regression lines

Another way to present the results, was by calculating the gradient of the regression lines. A summary of the gradients is shown in figure 4.10. Showing the gradients made it possible to spot the major model sensibilities and to understand its behavior. While changes in the unit weight had a neglectable effect on the runout deposit, the friction coefficient had the highest influence on it. Therefore the friction coefficient f is the Voellmy parameter which needs to be adjusted in order to achieve major changes in the runout. The turbulence coefficient and internal friction angle may be useful for small adjustments. Table 4.8 shows a summary with magnitudes of correlation between the parameter and runout results. The symbols used in table 4.8 represent the following: + positive correlation; - negative correlation; ∅ no correlation; / independent.

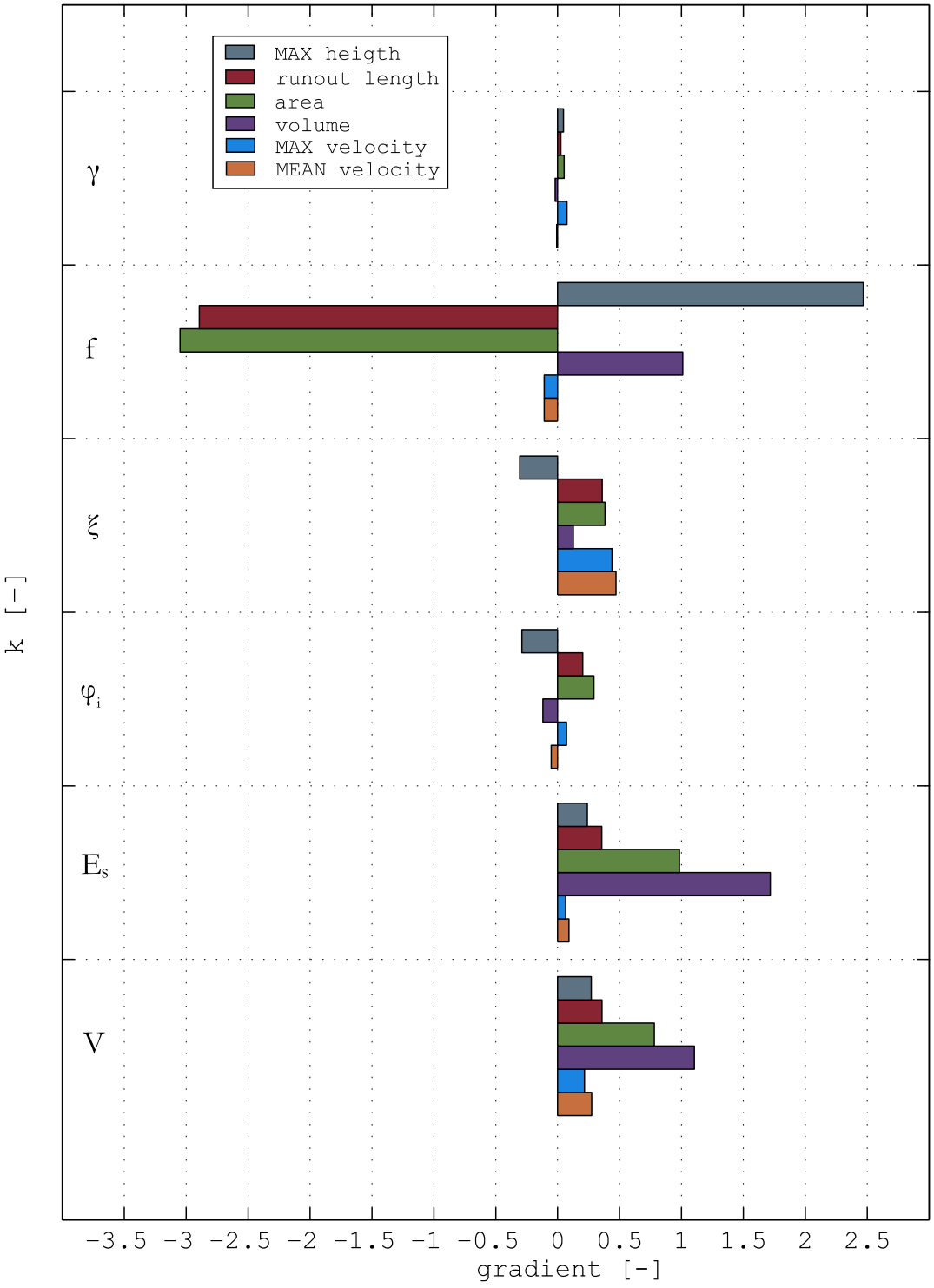

Figure 4.10 – Gradients of the regression lines

Table 4.8 – Correlation of the Voellmy parameters with the runout results

	RL	max h	A	V	MAX v	MEAN v
γ	/	∅	/	/	∅	/
f	-	+	-	+	/	/
ξ	+	-	+	+	+	+
ϕ_i	+	-	+	-	∅	-
E_s	+	+	+	+	+	+
V	+	+	+	+	+	+

4.4.8 Deposits of each computation

The following figures show the deposits from the sensibility analysis at the timestep t = 240 s. Only the first, center and last computation of each parameter study result are plotted.

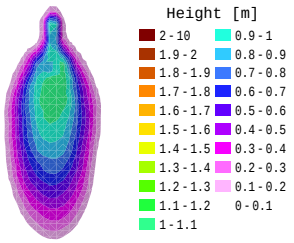

Figure 4.11 – Deposit a 01 ($\gamma = 13$ kN/m^3)

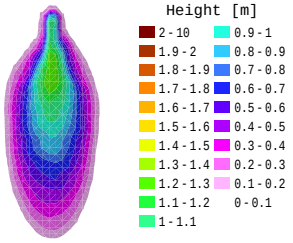

Figure 4.12 – Deposit a 06 ($\gamma = 18$ kN/m^3)

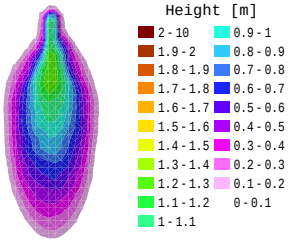

Figure 4.13 – Deposit a 11 ($\gamma = 23$ kN/m^3)

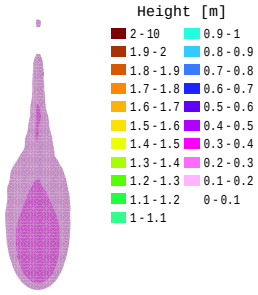

Figure 4.14 – Deposit b 01, half scale ($f = 0.08$)

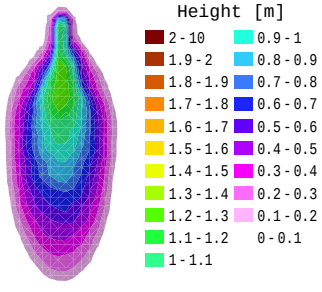

Figure 4.15 – Deposit b 05 ($f = 0.12$)

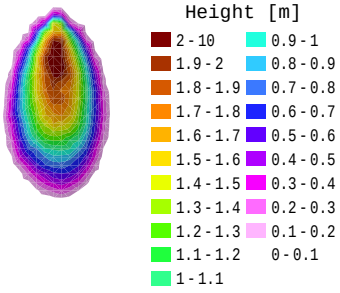

Figure 4.16 – Deposit b 09 ($f = 0.16$)

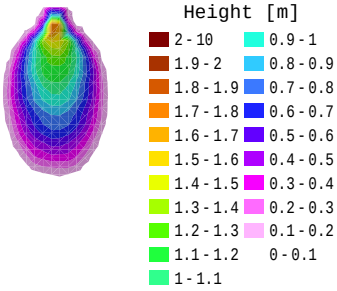

Figure 4.17 – Deposit c 01 (ξ = 100 m/s^2)

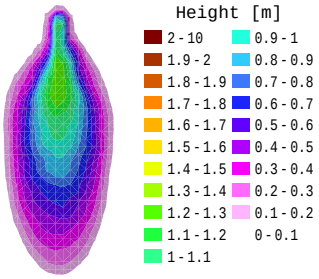

Figure 4.18 – Deposit c 05 (ξ = 500 m/s^2)

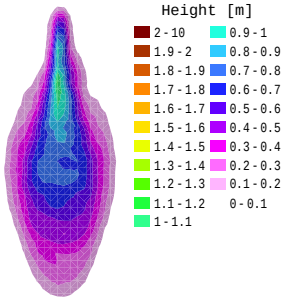

Figure 4.19 – Deposit c 10 (ξ = 1000 m/s^2)

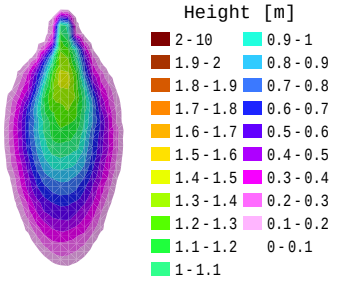

Figure 4.20 – Deposit d 01 (ϕ_i = 10°)

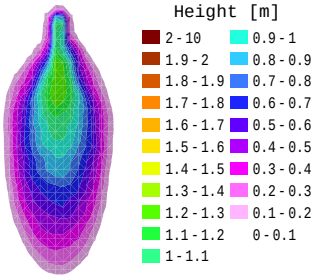

Figure 4.21 – Deposit d 05 (ϕ_i = 18°)

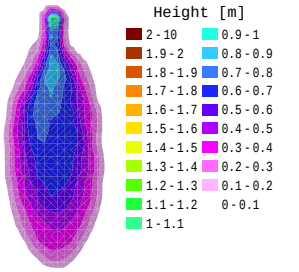

Figure 4.22 – Deposit d 11 (ϕ_i = 30°)

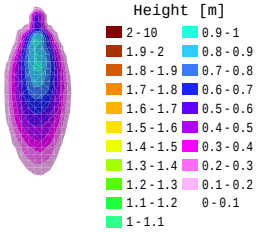

Figure 4.23 – Deposit e 01 (E_s = 0.00000 m^3/m)

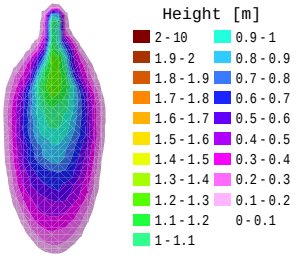

Figure 4.24 – Deposit e 07 (E_s = 0.00064 m^3/m)

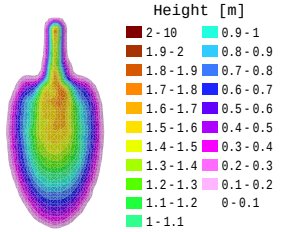

Figure 4.25 – Deposit e 10, half scale (E_s = 0.00184 m^3/m)

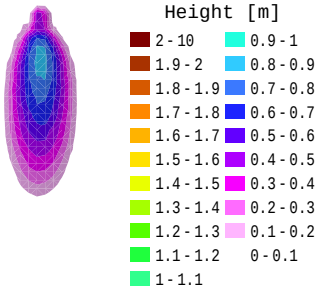

Figure 4.26 – Deposit f 01 (V = 750 m^3)

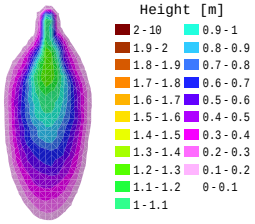

Figure 4.27 – Deposit f 05 (V = 2250 m^3)

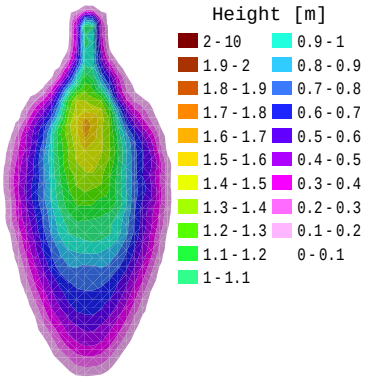

Figure 4.28 – Deposit f 11 (V = 4500 m^3)

Chapter 5

Back-analysis and prediction

5.1 Introduction

Predicting physical behavior in the future is a common engineering problem. In terms of risk assessments, future events with a small probability of occurrence need to be modeled. This is probably the major and most important application of a debris flow model. Unlike in other engineering fields, the knowledge for the prediction of debris flows is still under development. The parameters which need to be set in the model cannot be measured in the laboratory or on-site and the debris source and maximum erosion depth are mostly unknown. A back-analysis of past events is needed to calibrate the model.

5.2 Back-analysis

A back-analysis models the behavior of an event that has already happened. The purpose is to evaluate the unknown parameters with which the model fits best the real event. Certain data need to be available in order to achieve a reliable back-analysis. Most important are the debris source, deposit and erosion information. If these data are available, and if so, how certain they are, rules the success of a back-analysis.

A good event documentation can provide the user with data about the exact source extent and volume, erosion depths, deposit area, deposit height and deposit volume. Furthermore, the duration of the event and pictures of it will increase the depth of information. Using all these data should provide enough information to create the input grid files for

DAN3D.

Due to the fact that available event data are not always accurate or even available, the grid files need to be created from all available "Hard" and "Soft" data. The following descriptions are based on the author's experience on the back-calculation of the "Seefeldbach" debris flow. If the data are provided in other formats or depths of information, other strategies may need to be developed.

5.2.1 "Hard" and "Soft" data

The documentation of a debris flow event or any other bigger landslide consists of both "Hard" and "Soft" data. "Hard" data are all those, which were measured on-site and stored in a way that they can be reproduced exactly. GIS data of the pre or past-event topology can be defined as such. "Soft" data are information which can be used to improve existing "Hard" data. For example on-site pictures of the deposit can be used to get an idea about the range of the deposit depth, but cannot be used to reproduce exact numbers. A proper distinction of the given data in these two categories and a clever intersection is essential for it. If the analysis of the data and the following preprocessing do not match the real properties, further parameter estimations are without any meaning.

5.2.2 Preprocessing

The following subsections describe the workflow creating the input grid files for DAN3D using available event data.

Path topography

This grid file describes the pre-event three dimensional terrain. Therefore three dimensional GIS information older than the event can be used for this purpose. The accuracy and resolution of this 3D terrain compared to the dimensions of the debris flow has a major influence on the model performance. This sensibility increases with smaller debris flows and more complex terrain.

Source

The evaluation of the source file is probably the most uncertain process of the whole back-analysis procedure. The heights of the debris source and its extents are required. Thus an exploration of the geological conditions is absolutely necessary. Debris flow events are often built up by several side-streams, and it is difficult to estimate the exact source area and depth. It can be transformed to a source grid file, if there are correct GIS data available about the source. Generally there will be no source grid file available and the user needs to evaluate it by "soft" data. This means that using event and pre-event pictures, orthofoto and maps indicating the event boundaries should provide enough information to create at least the extent of the source. In some cases, the depth can be estimated by analyzing on-site pictures, event descriptions and geomorphological information. If this information are not sufficient, an on-site survey needs to be carried out.

Erosion

This grid file describes where erosion is possible and what is their maximum depth. Normally there is erosion along the whole debris flow path. Analyzing pictures or reports of the event can help to evaluate the erosion depths. Using geological indications about the depth of erodible material would provide even better information. The erosion depth should be controlled by the model parameter "erosion rate" and not with the maximum erosion depth. If the volume of the flowing material is not big enough, the erosion will stop before reaching their maximum depth.

5.3 Prediction

The prediction of a future event still has many uncertainties. Not only are the model parameters almost unknown, but most importantly the source is unknown. Without a certain knowledge of the size, location and volume of the debris material, no reliable predictions can be made.

5.3.1 Prediction of the source

There are many possibilities to predict the source volume and position, but none of them produces reliable results. Due to the complexity of such a problem many different approaches are presented in literature. Two examples are shown in the following two paragraphs.

On-site estimation - empirical method

It is possible to do a simple estimation of the volume and position of loose and transportable debris. The estimation could be made by an on-site visit using simple measures. By analyzing on-site pictures with the estimated debris depth, it is possible to draw the source area onto orthofotos. This information can be combined with its depths which leads to the source volume. This procedure is very uncertain and there is no justification for when and how much of the material can be mobilized. Therefore this approach is used cautiously and it probably overestimates the real source volume. It is also possible to use only the orthofotos in combination with geological maps, but probably more uncertain than on-site measures. The users's experience with debris flows and defining their sources plays a key role for this method.

Physical relationships - analytical method

Another way to predict a source volume is by modeling seepage and infiltration combined with a GIS soil stability analysis (Jakob et al., 2005). Pack et al. (1998) and Montgomery and Dietrich (1994) presented the Software SINMAP and SHALSTAB respectively, which combine physical relations about seepage, infiltration and soil stability based on Darcy´s law into a software bundle. They were designed to predict a shallow failure of steep slopes and perform the following computations: simple hydraulic computation of the steady-state pore pressure combined with an infinite slope analysis (Jakob et al., 2005). Using this tool can produce slope failures with a distinct volume, which are in fact the debris flow sources.

5.3.2 Setting model parameters

The model parameters of DAN3D cannot be calibrated using laboratory or on-site tests (McDougal, 2006) and therefore rely on values gained from experience. Performing back-analysis of different events and personal experience with the software may help to choose the model parameters. Ayotte and Hungr (2000), Chen and Lee (2003b) and Pirulli et al. (2004) have developed ranges of model parameters. They are bundled by Sosio et al. (2008) in a table where the range of model parameters is given for different landslide types. It shows the following parameter range for debris flow events:

- frictional rheology: internal friction angle $\phi_i = 35°$, bulk friction angle ϕ_b = 22-29°;
- Voellmy rheology: internal friction angle $\phi_i = 35°$, frictional coefficient μ = 0.05-0.2, turbulence coefficient ξ = 200-500ms^{-2};

Another promising approach was derived by Ayotte and Hungr (2000) but it is only available for rapid rockfalls. After the back-calculation of many different rockfall events, the authors showed that using a Voellmy rheology with a friction coefficient of $f = 0.1$ and a turbulence coefficient $\xi = 500$ m/s^2, 90% of the events had a shorter runout length than predicted. Using these parameters a reasonable first order prediction can be made. It is unclear if these values can be adopted to a debris flow model, but the results of the following chapter 6 may give answers to that.

Chapter 6

Modeling the "Seefeldbach" debris flow

6.1 Introduction

The "Seefeldbach" debris flow happened on July 13^{th}, 2002 in the village of Mühlwald, located in the north eastern part of South Tyrol - Italy. Heavy rain triggered this event where the debris flow reached the valley river, and probably overflowed it on its east side. It is assumed that the debris consisted of eroded morain.

The infrastructure and houses (so called "Wassermannhof") along its deposition area were damaged heavily. Two debris flows with connected deposition areas were happening simultaneously. In order to simplify the modeling process and to focus on the proper evaluation of the grid files and model properties, only the longer debris flow which started from the peak of the mountain was modeled. Therefore the deposit volume should be smaller than the on-site estimated volume, but there is no possibility to evaluate the exact number. The following sections describe the back-analysis of this event including the preprocessing of the event data, calibration of the model and finally a discussion of the results. Voellmy and frictional resistance will be used for the basal shear resistance.

6.2 Location

Figure 6.1 shows the topography of the eastern part of South Tyrol, indicating the study area with a black circle. Mühlwald is located in the valley "Mühlwaldtal" which is a side-valley of the "Ahrntal", a side-valley of the "Pustertal". Figure 6.2 and figure 6.3

show the orthofoto and topography of the study area in detail.

The Mühlwaldtal is a narrow valley surrounded by steep and high mountains. The "Seefeldbach" valley begins at about 2100 m and ends at 1300m. The slope of the valley varies between 50 % to 60 % and the slope of the deposition zone is approximately 15 %. The software ArcGis was used to create a "steepest path", starting at the top of the source area and finishing at the valley river. The plan view and longitudinal section of this analysis is shown in figure 6.3 and 6.4.

Geologically the Mühlwaldtal is located in the "Altkristallin" (series of metamorphic rocks). The study area consists of Paragneiss, Gneiss, moraines mixed with debris and detritic cones with alluvial cover. A geological map of the study area is shown in figure 6.5.

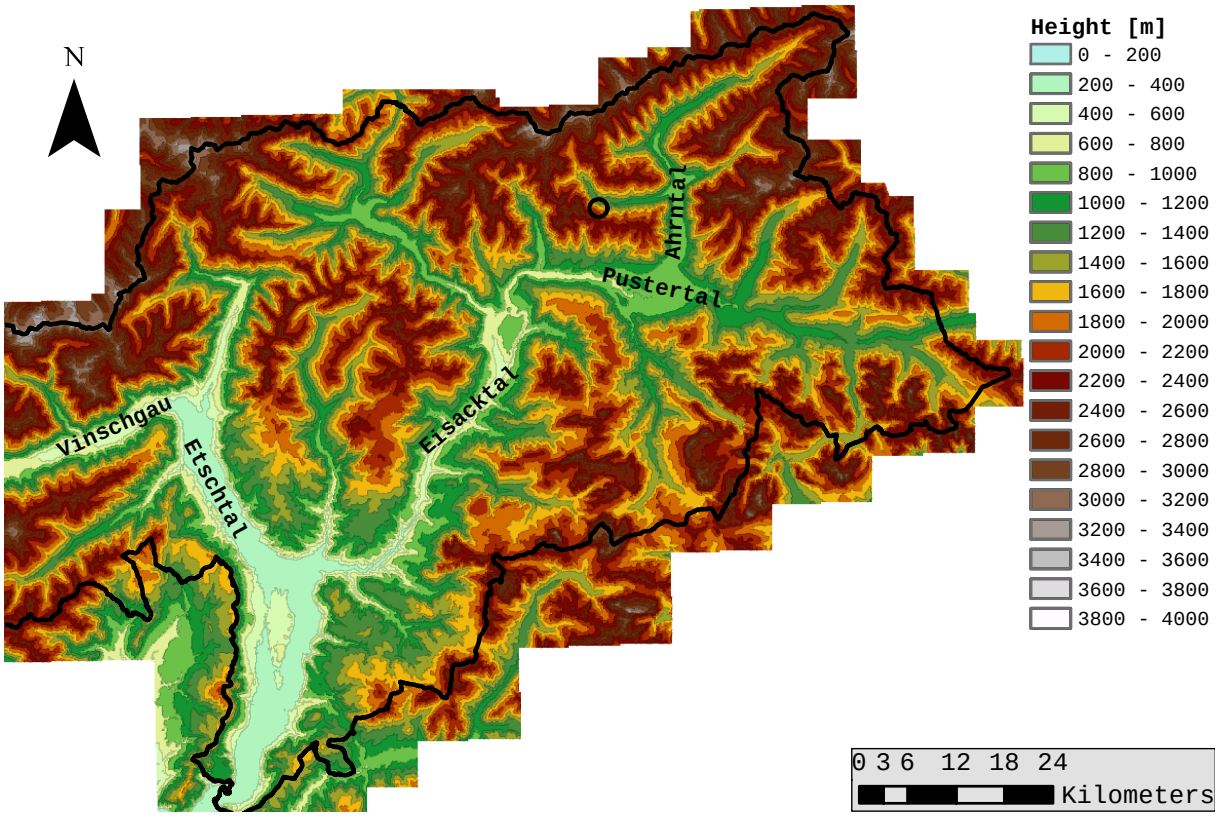

Figure 6.1 – Topography of the eastern part of South Tyrol - scale 1:1.000.000

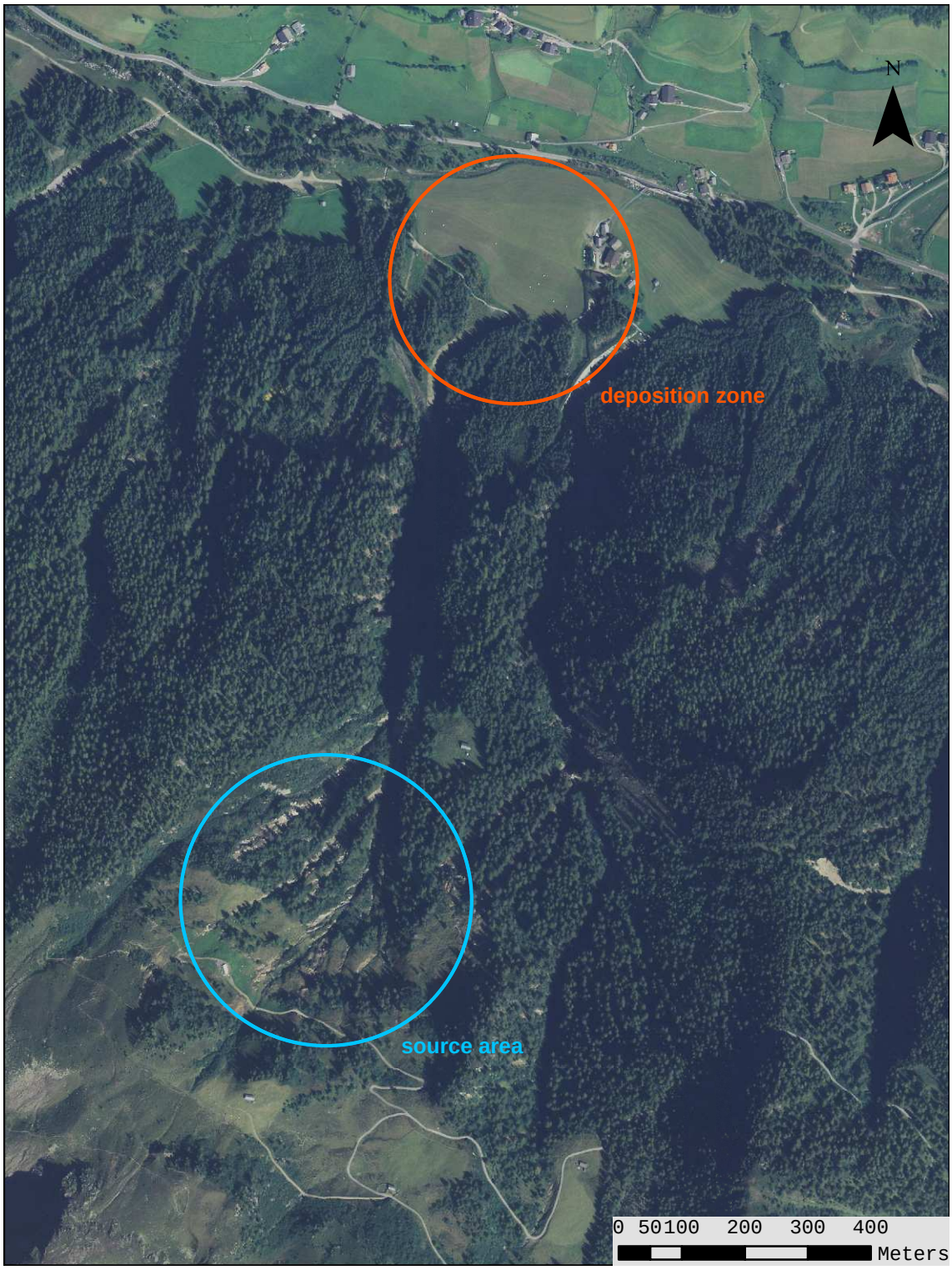

Figure 6.2 – Orthofoto of the study area - scale 1:10.000

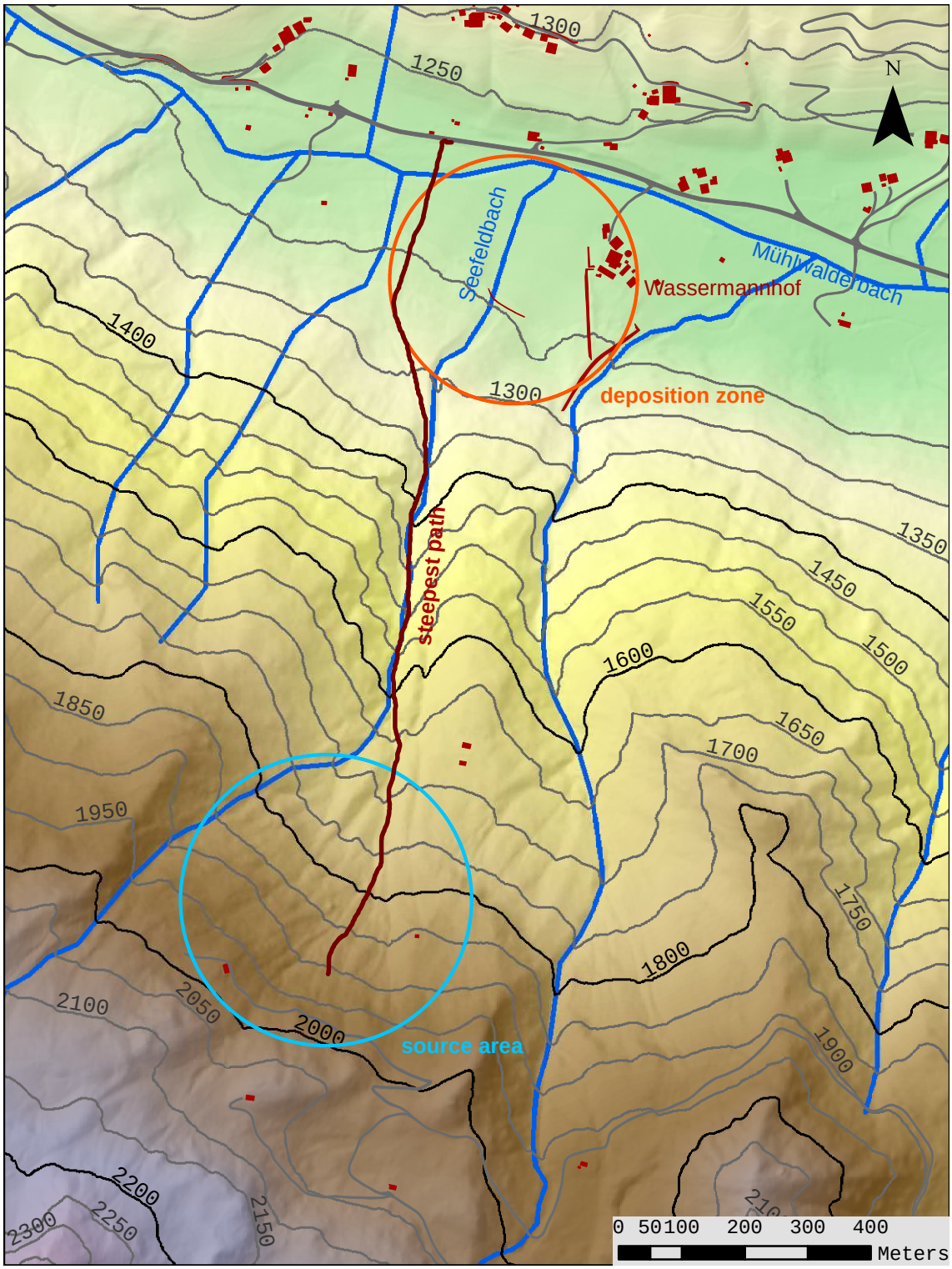

Figure 6.3 – Topography of the study area including a steepest path- scale 1:10.000

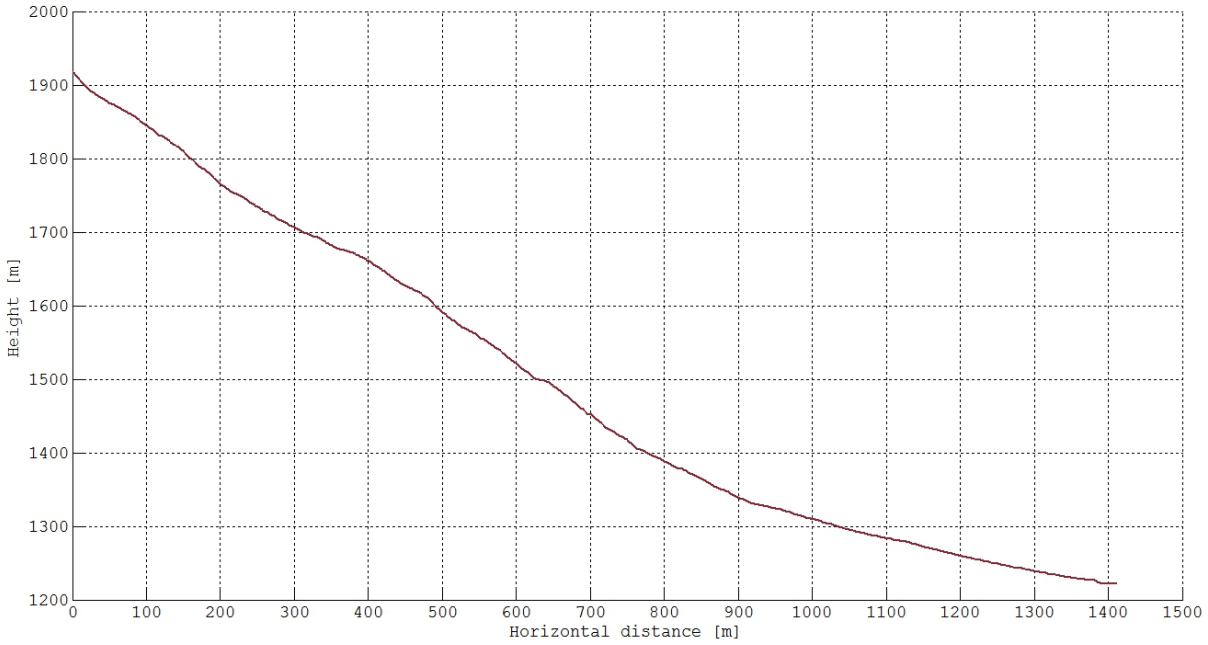

Figure 6.4 – Longitudinal section of the steepest path shown in figure 6.3 - scale 1:10.000

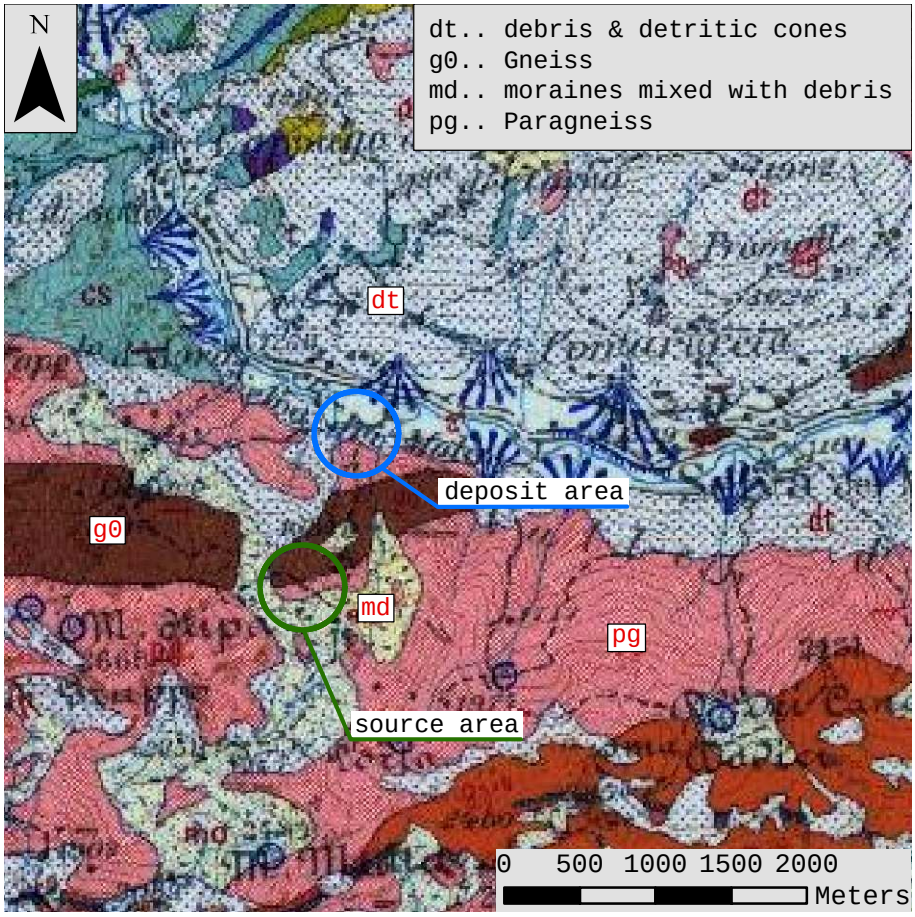

Figure 6.5 – Geological map of the study area - scale 1:50.000 (created on the base of the geological map of South Tyrol (Abteilung11.6, 2011))

6.3 Event data

The event data can be categorized into incident data and local topography information.

6.3.1 Incident data

The office "Wasserschutzbauten" (Abteilung30, 2010) of the province of South Tyrol - Italy provided debris flow datasets for this thesis. It includes photographs of the incident, annotations about the event and shape files of the source, the path and the deposition zones. Depending on the engineer that worked on-site, the data has different depths of information. This is notable because in some cases the data lacks information and accuracy.

Photographs were taken immediately after the event of the debris flow path and the deposit zones. They provided qualitative information ("Soft data") about the size and power of the debris flow, damage resulting from it, debris compositions, deposits, source and entrainment dimensions.

Annotations are available for all incidents in form of a standard handout. These handouts are implemented in the incident documentation ED30 made by the institution "Wasserschutzbauten". Every incident has its own number, and provides at most the following information: code of the event, type, date, zonal area, objector,affected reach, what kind of infrastructures was harmed (e.g. private houses, agriculture areas, commercial areas etc.), meteorologic conditions, starter mechanism, description of the grain distribution, deposit description (volume, medium height, volume of wood) and additional notations.

Shape files in the ArcGis format are available for all documented incidents of the province. The point shape files describe the location, points of damage, direction and place where the photographs were taken, debris source, debris deposition and entrainment zones of the debris flow. The line shape files are not really helpful because they provide almost the same information as the polygon shape files. The polygon shape files provide information about the area of the source, erosion zones and deposit areas. The deposits are divided into zones with different heights. It should be mentioned that these shape files were created from poor observation data, which in most cases was only an on-site estimation. Therefore all shape files need to be considered as qualitative information which needs to

be improved by other data and logical conclusions. Consequently, most information needs to be evaluated using the event pictures.

Figure 6.6 – Aerial view on the debris flow deposit
from Abteilung30 (2010)

Figure 6.7 – on-site view on the debris flow deposit
from Abteilung30 (2010)

Figure 6.8 – Bed erosion along the main path
from Abteilung30 (2010)

Figure 6.9 – Aerial view on the debris flow source
from Abteilung30 (2010)

The main geological type in this area is the "Altkristallin". Some

6.3.2 Terrestrial information

The terrestrial information can be taken from a DEM. This has been provided by the provincial office "Raumordnung" (Abteilung27, 2010) and can be downloaded for free on their website. The DEM was created in 2005 with a LIDAR observation (a laser scan taken from an airplane) and is available in form of a ArcGis ASCII grid file in a density of 2.5 m x 2.5 m. The coordinates are defined in the ETRS89/UTM reference frame and have a minimal height accuracy of 25 cm in well documented ares (where a technical map in a scale of 1 : 5000 is available), 40 cm in poorly documented areas and 40 cm where the terrain is higher then 2000 m.

Furthermore another DEM is available, which was created in 2000, but testing this data has shown that it is too imprecise for using it in further investigations.

Another source of information are orthofotos, which are available for the whole province (Abteilung27, 2010). Two sets of orthofotos are available, both made by aerial photog-

raphy in a scale of 1:10.000. The first set was made between summer and fall 1999, has a maximum information depth of 4m and is colored in a gray scale. The second set was taken in the summer of 2006, it has a minimal resolution of 0.5m and is colored. The latter will be used for the preprocessing of the input grid files.

6.4 Creation of the input grid files

6.4.1 Source grid file

At first the area and depth of the debris flow source needed to be evaluated. Due to the fact that the polygon shape files of the events are not very accurate, it was chosen to redraw them by using terrestrial maps, orthofotos and the DEM. This was performed in AutoCad Map by drawing polylines around the detected sources. In fact this step is questionable, because it was just drawn by hand. However there is no better way to get this source area, and the photos taken after the event give a reasonable good information about the positioning and size of the areas. The orthofotos, DEM and technical map were placed underneath the drawing and helped to assign the areas.

The next step was to identify the depth of the source areas by analyzing the photos and making reasonably assumptions. It was decided that the source has an approximate maximum depth of 1.2m. After completion of these steps, so called MPOLYGONS were created from the polylines. The height of these polygons was added using an ArcMap like attribute table. After these steps, polygons with equal height of source were exported as a ESRI shape file. This shape file was transformed to a ESRI grid using the software ArcGis. Finally this grid was loaded into the software Surfer and was transformed into the required ASCII GRD grid file.

6.4.2 Topography grid file

Normally this file should be created from a pre-event DEM where the source of the debris flow was subtracted. No sufficiently accurate DEM before the event was available. Therefore the 2005 DEM builds the basis for the path topology grid file. By definition of the path topology grid file, the source volume needs to be subtracted from the original

path. In our case we already had the exposed rupture surface by using a post event DEM. It was not possible to recalculate the proper pre-event DEM heights. Therefore some error in the results is to be expected. After the event, the government organization "Wasserschutzbauten" increased an earth dam on the end of the torrent valley which was to prevent future debris flows to damage the houses again. The torrent basin, which leads from the dam to the valley rive, was probably also improved. There was no data available about the dimensions of these measures and therefore they could not be implemented into this grid. This generates another source of error.

6.4.3 Erosion grid file

There was no proper information about the extent and depth of the erosion along the debris flow path. Event pictures were analyzed and gave an indication of the maximum erosion depth of 2 m limited by the bedrock.

6.5 Back-analysis

The major goal for this back-analysis was to fit the runout deposits to the real event. Therefore a polygon file of the real deposit was created which could be overlaid on top of the model results. Figure 6.10 shows the source contours and the real event deposit boundary.

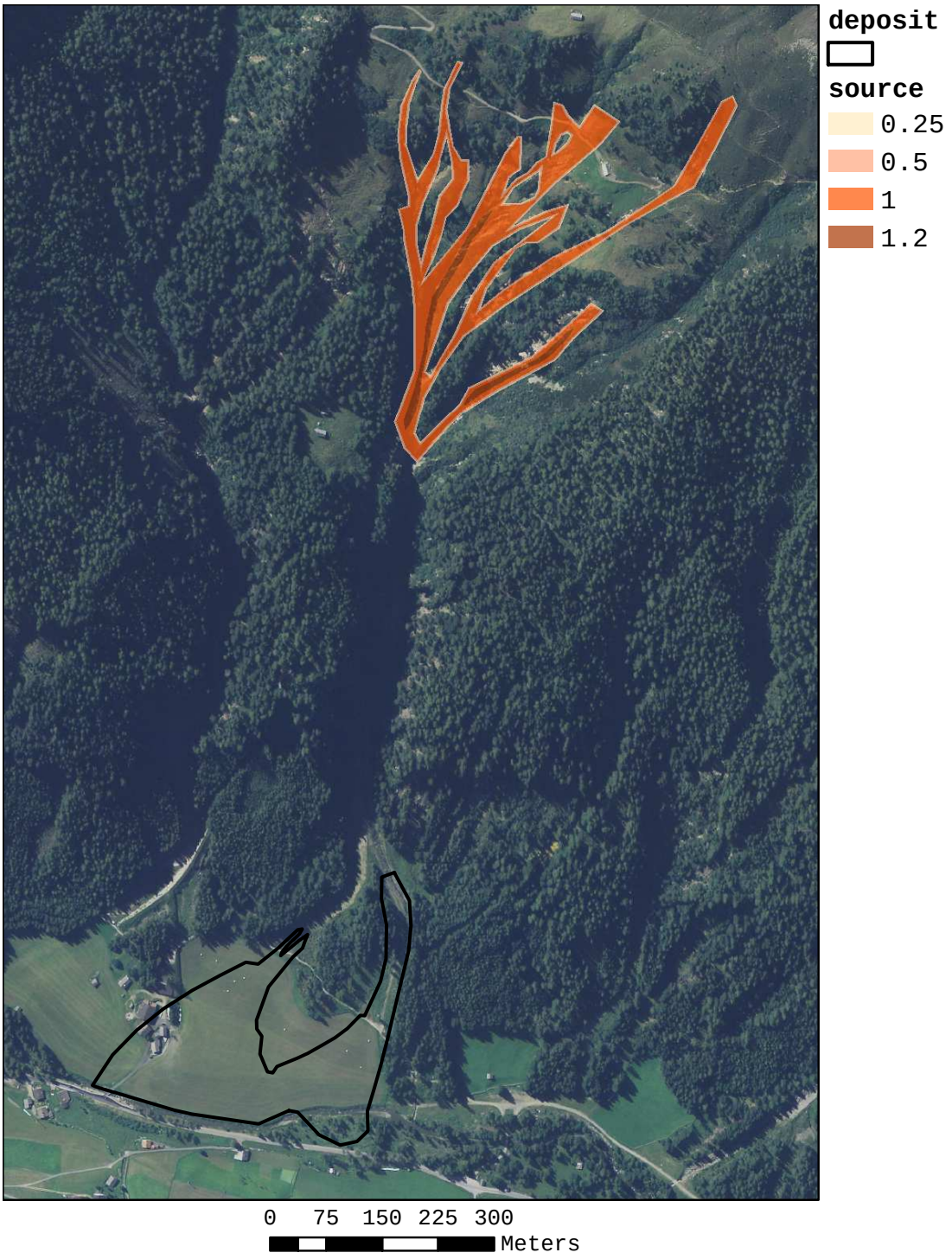

Figure 6.10 – Orthoview of the Seefeldbach source and deposit

It was tried to model the debris flow using the Voellmy and frictional rheology. Using the knowledge gained from chapter 4, the parameter variation was performed using the friction coefficient for the Voellmy rheology and the bulk friction angle for the frictional rheology.

6.5.1 Back-analysis using the Voellmy rheology

Model parameters

According to the results of chapter 4, this back-analysis tried to fit the model by variation of the friction coefficient f. The rest of the parameters were set to the following values: $\gamma = 18$ kN/m^2, $\xi = 500$ $\frac{\text{m}}{\text{s}^2}$ and $\phi = 18°$. A summary of the used friction coefficient f for 9 models is shown in table 6.1.

Table 6.1 – Friction coefficient f

Nr.	1	2	3	4	5	6	7	8	9
f	0.115	0.110	0.105	0.100	0.095	0.090	0.085	0.080	0.075

Results

All results show a good fit to the overall event properties. The deposits of each model are shown in figure 6.11 to figure 6.19

The debris fan divides into two streams shortly before the deposition area. Due to the slightly wrong topography in the deposition area the orographically left debris fan travels too far to the left. Model 4 which uses a Voellmy parameter $f = 0.100$ delivers the best fit result and is shown in figure 6.14. The area of the orographically right debris fan fits quite well the real event area. The maximum height of that side is about 2.5 m and smoothly spreads over the area. DAN3D performed well on reproducing the event, with the exception of the error on the orographically left side, which is probably caused by the previously described errors in the pre-event DEM.

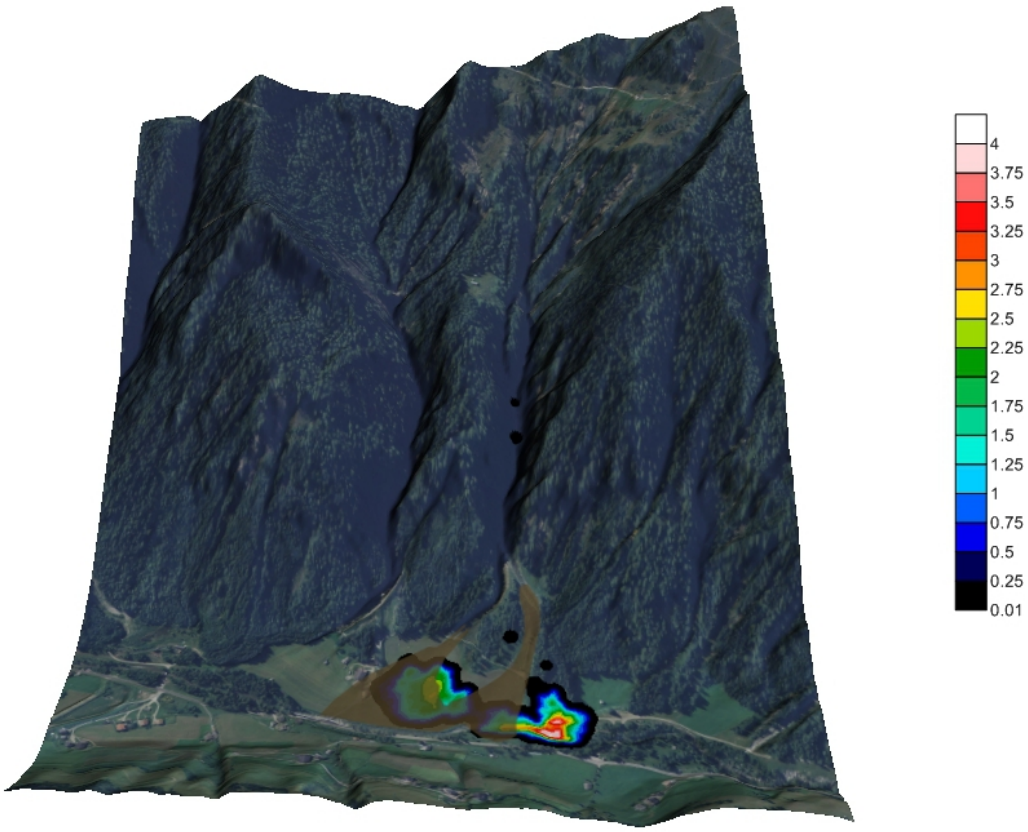

Figure 6.11 – Resulting deposits using $f = 0.115$ and $\xi = 500$ m/s^2

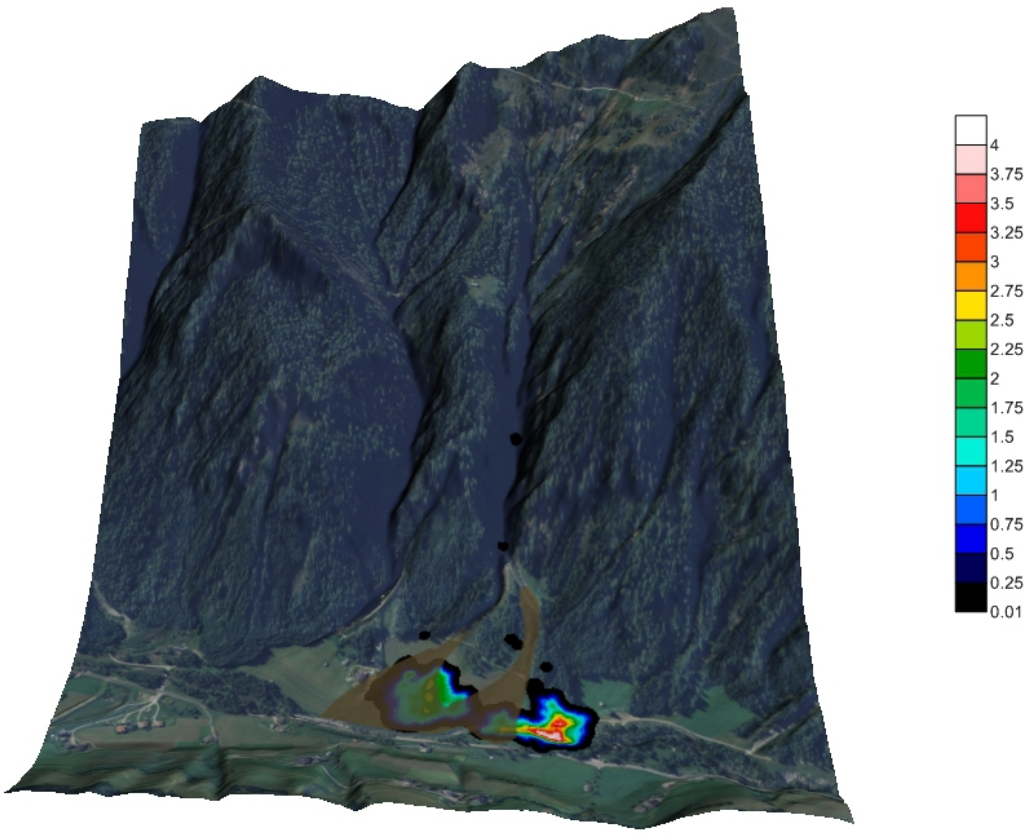

Figure 6.12 – Resulting deposits using $f = 0.110$ and $\xi = 500$ m/s^2

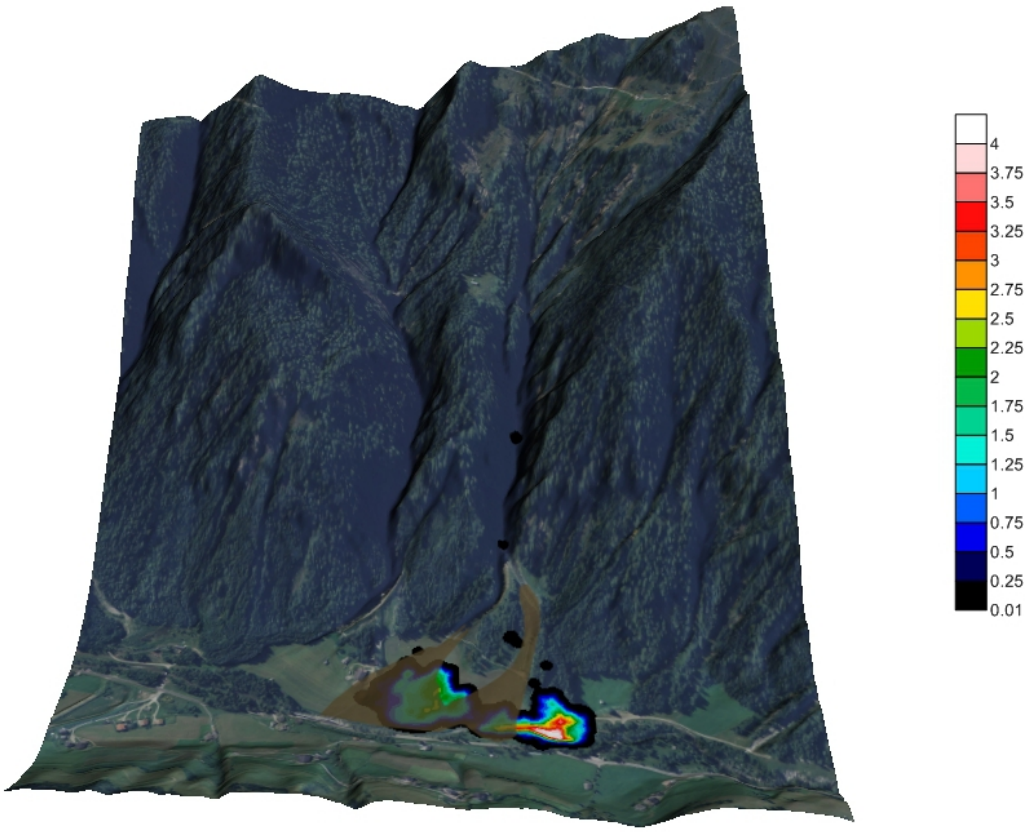

Figure 6.13 – Resulting deposits using $f = 0.105$ and $\xi = 500$ m/s^2

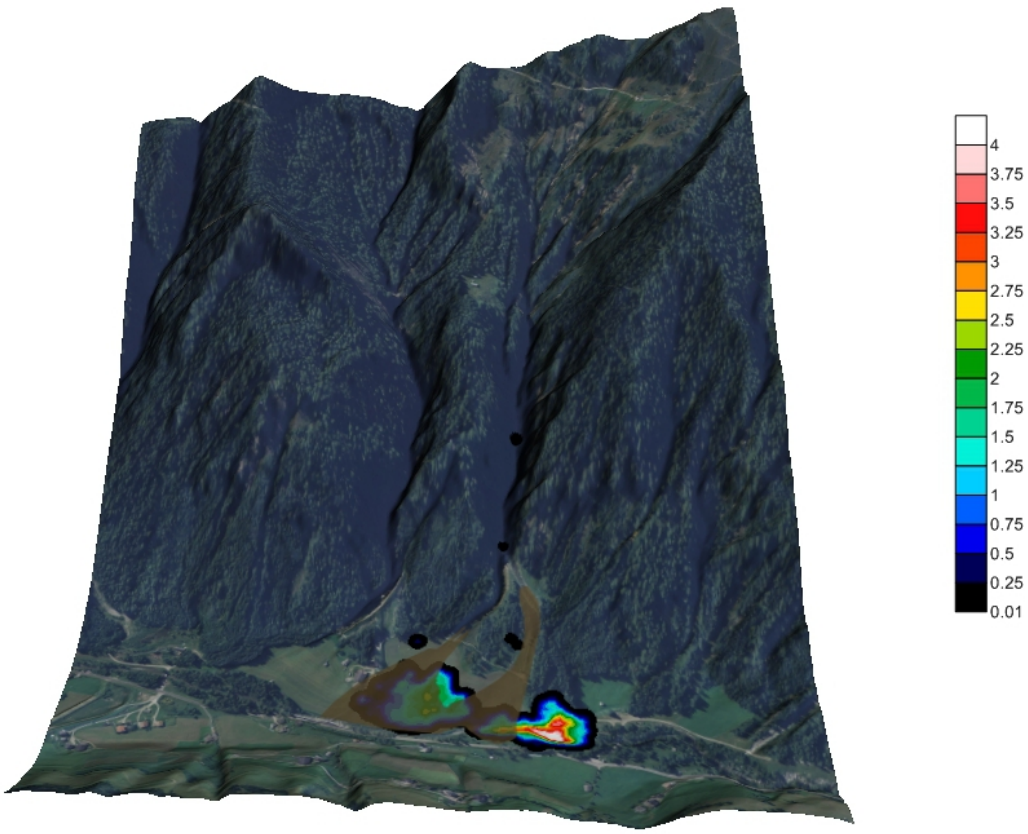

Figure 6.14 – Resulting deposits using $f = 0.100$ and $\xi = 500$ m/s^2

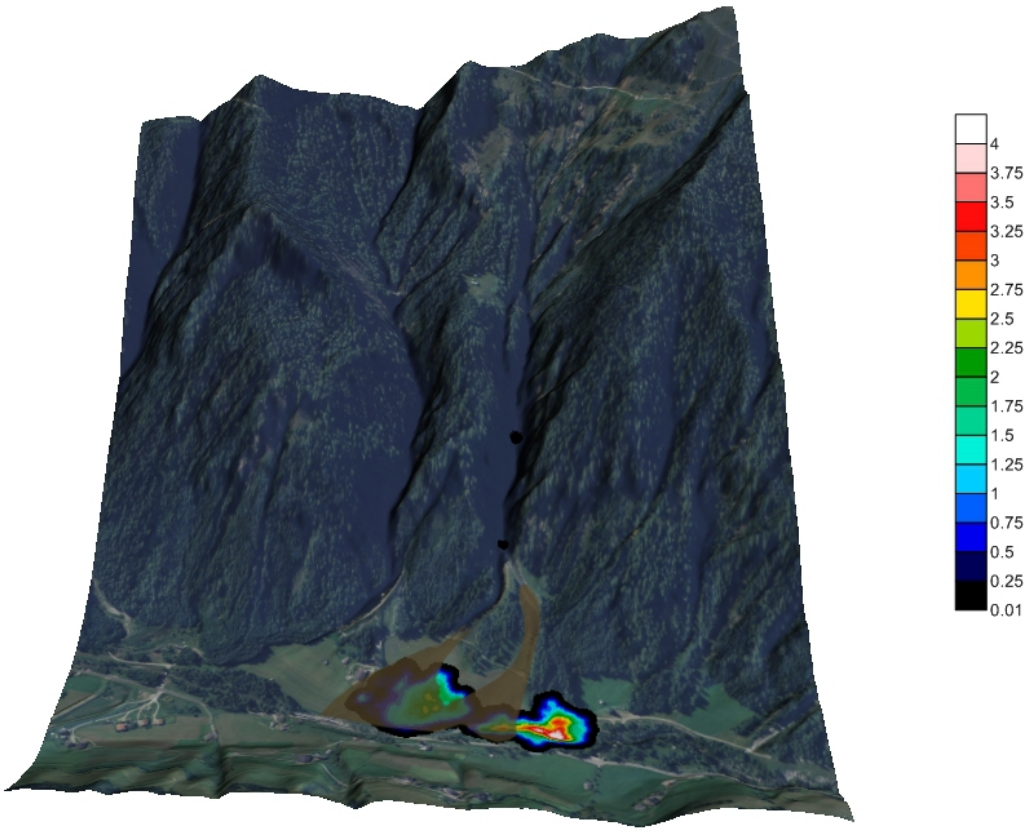

Figure 6.15 – Resulting deposits using $f = 0.095$ and $\xi = 500$ m/s^2

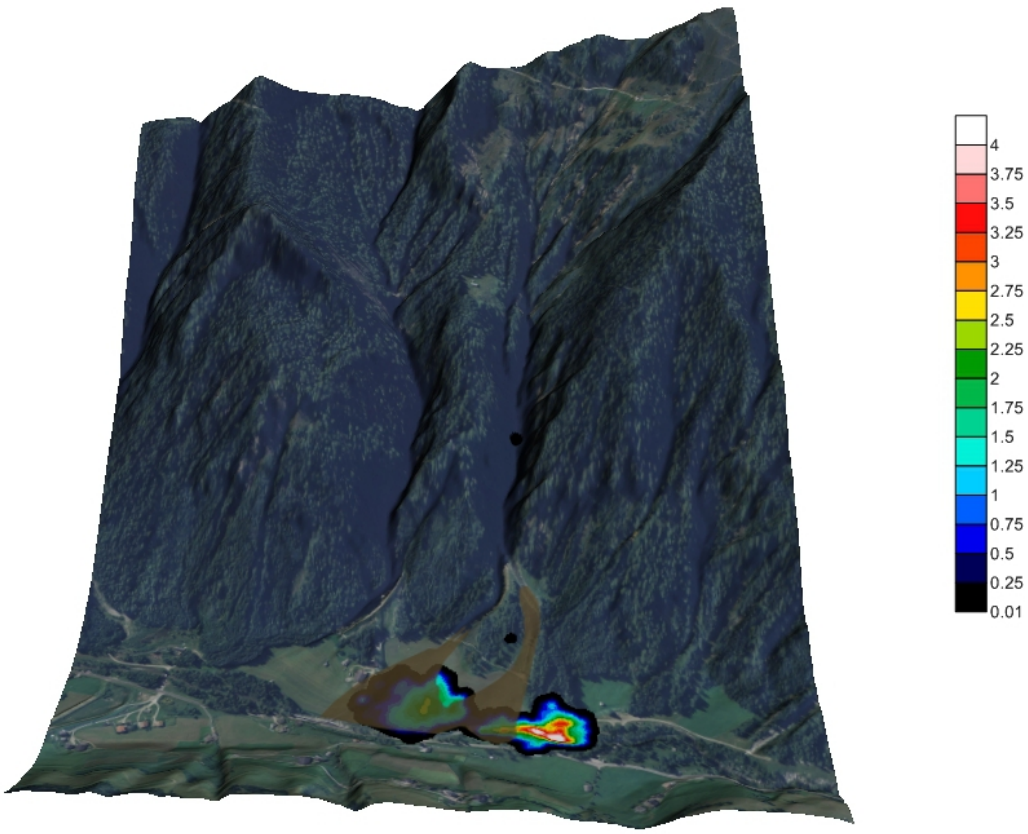

Figure 6.16 – Resulting deposits using $f = 0.090$ and $\xi = 500$ m/s^2

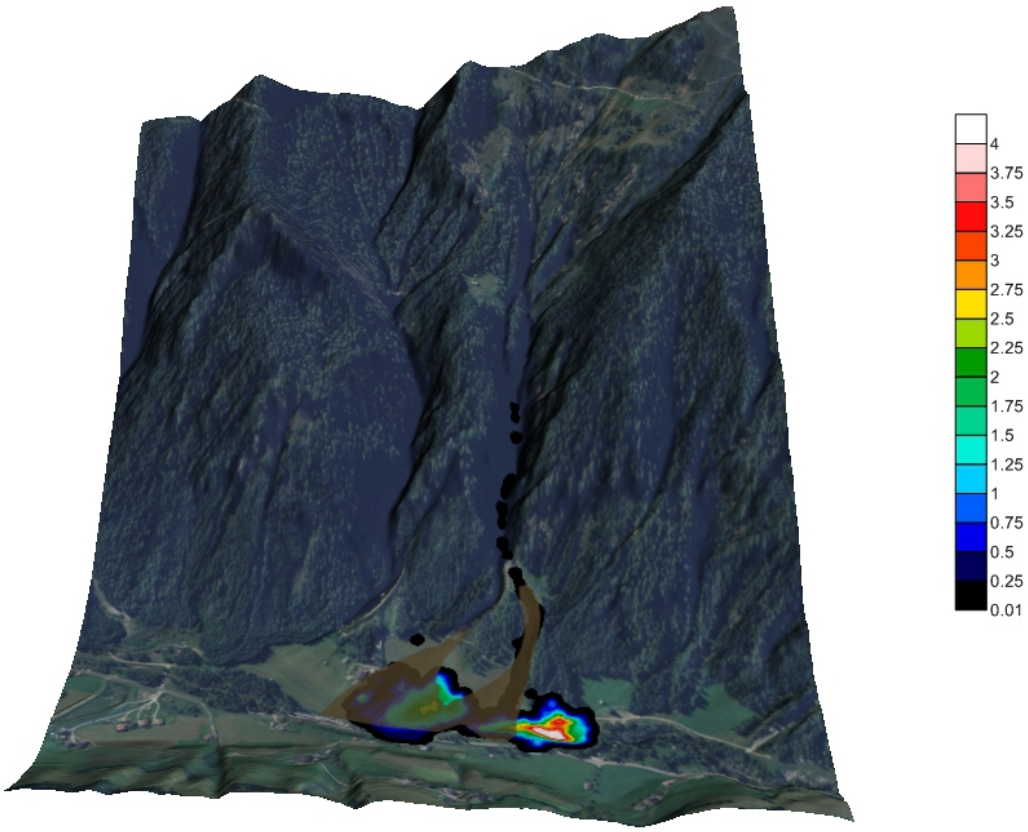

Figure 6.17 – Resulting deposits using $f = 0.085$ and $\xi = 500$ m/s^2

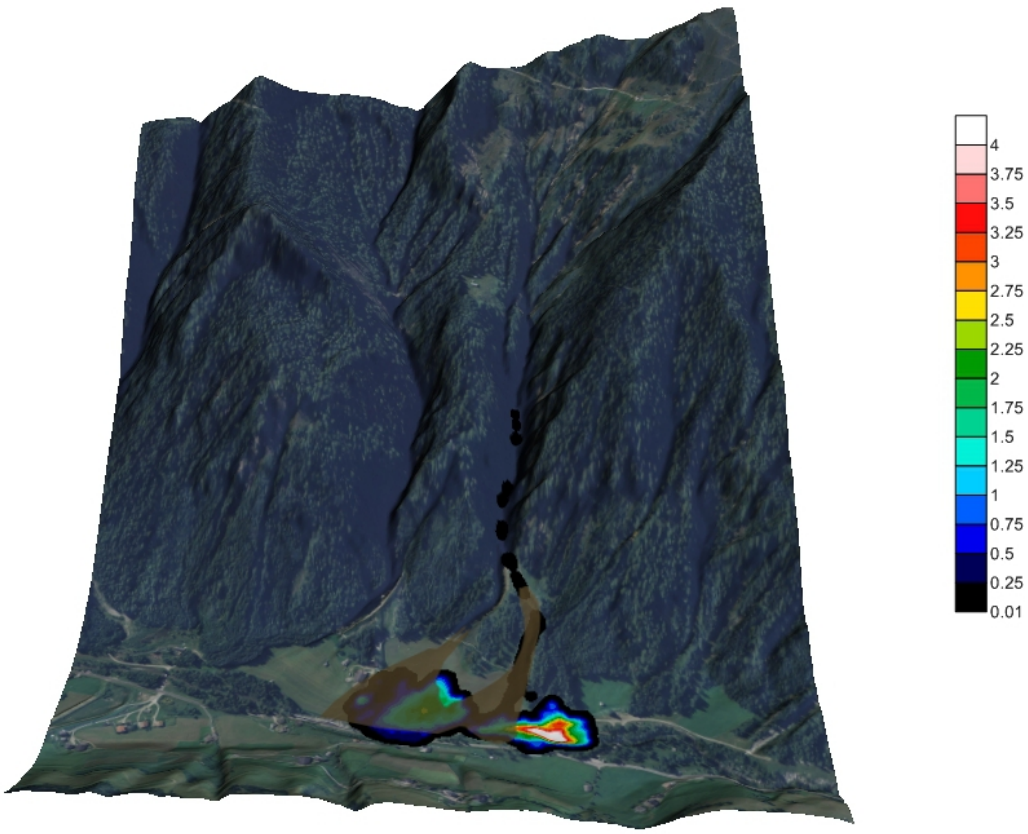

Figure 6.18 – Resulting deposits using $f = 0.080$ and $\xi = 500$ m/s^2

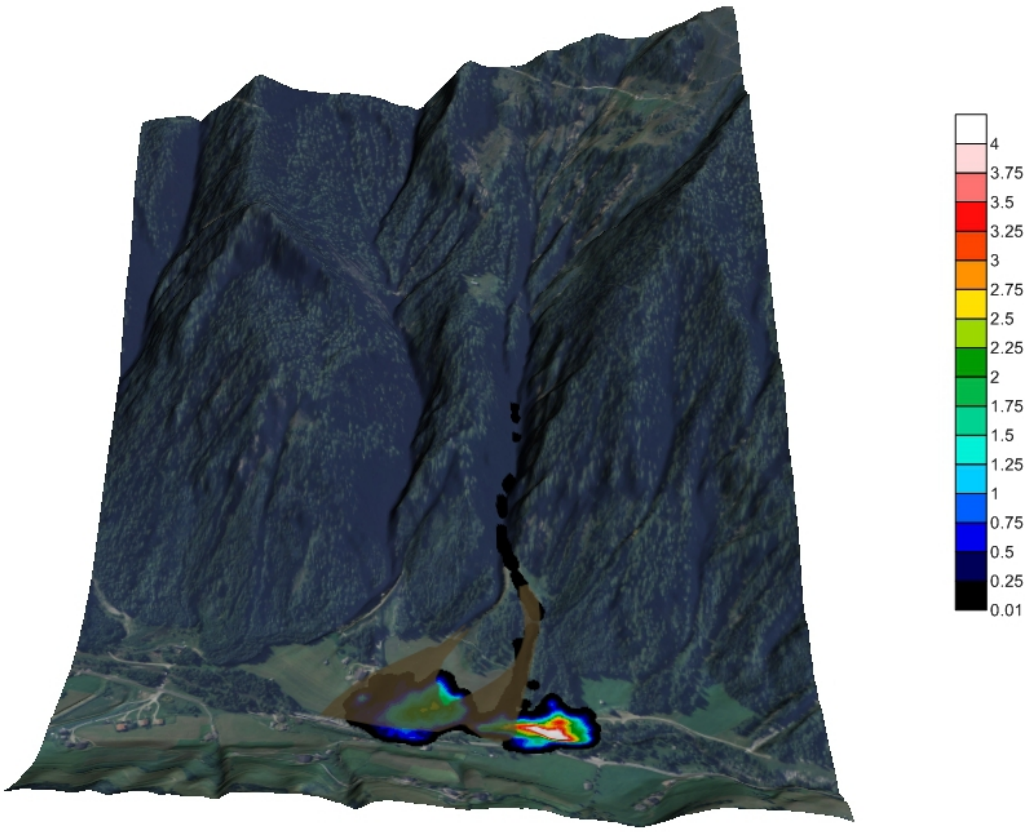

Figure 6.19 – Resulting deposits using $f = 0.075$ and $\xi = 500$ m/s^2

6.5.2 Back-analysis using the frictional rheology

For the frictional rheology several parameters needed to be predefined. The unit weight γ was set to 18 kN/m^2, the porepressure coefficient r_u to 0.5 and the internal friction angle to 18°. Previous calculations showed that this unit weight and internal friction angle lead to promising results. Debris flows in this region are triggered by heavy rainfalls. Therefore the assumption of completely wet soil can be justified. For this back-analysis, a range of the values indicated in table 6.2 were used in the following models. The indicated values of the bulk friction angle ϕ_b can be back-calculated to the needed basal friction angle ϕ using formula 6.1 from McDougal (2006).

$$\phi = \arctan\left[\frac{\tan\phi_b}{1 - r_u}\right] \tag{6.1}$$

Table 6.2 – Bulk friction angle ϕ_b and basal friction angle ϕ

Nr.	ϕ_b	ϕ
f01	10.0	19.4
f02	12.5	23.9
f03	15.0	28.2
f04	17.5	32.2
f05	20.0	36.1
f06	22.5	39.6
f07	25.0	43.0

Results

The results are shown in figures 6.20 to figure 6.26. They show the high runout dependency on the basal friction angle. Again the debris flow separates into two fans. The orographically left fan drifts too far to the left side like in the models using the Voellmy rheology. The debris travels too far using a bulk friction angle of 10.0° and 12.5°. On the other hand, the runout of the models f04 ÷ f07, stops before the real deposit area.

Model f03 with $\phi_b = 15°$ shows the best result and is shown in figure 6.22. The orographic right fan travels less uniform compared to the best fit Voellmy model. Also the maximum deposit height of over 3.5 m is too high. The deposit is too peaky around the maximum depth and too shallow on its boarders.

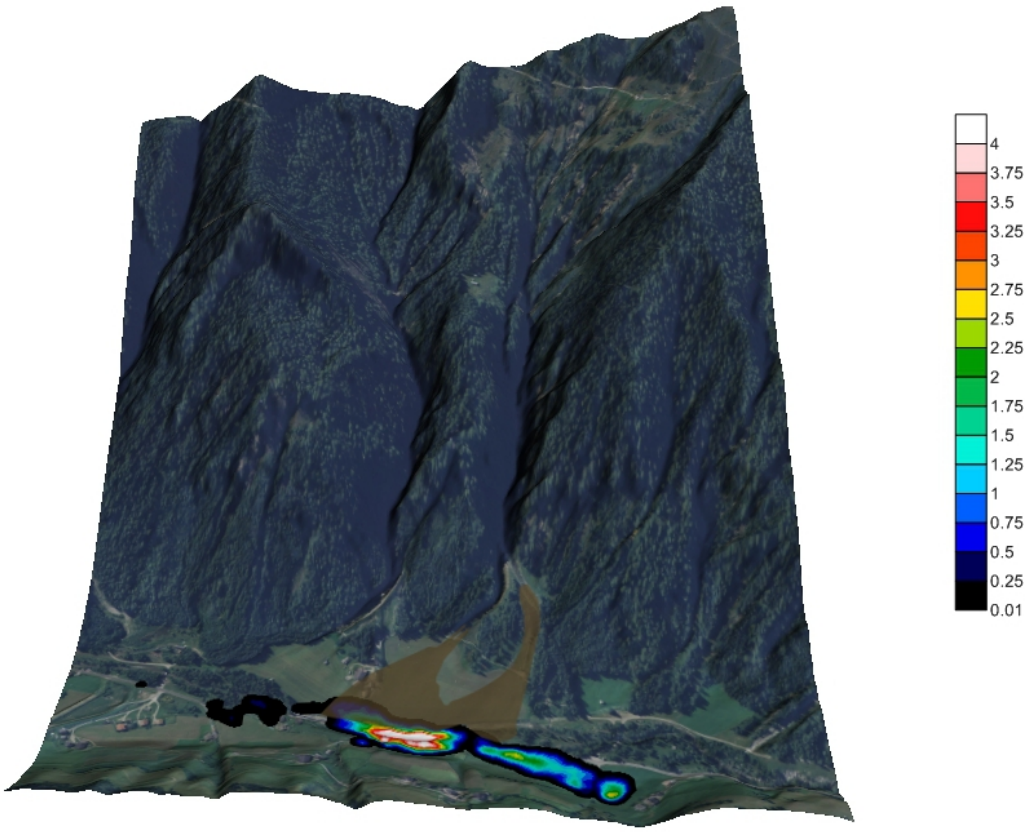

Figure 6.20 – Resulting deposits using $\phi_b = 10.0°$

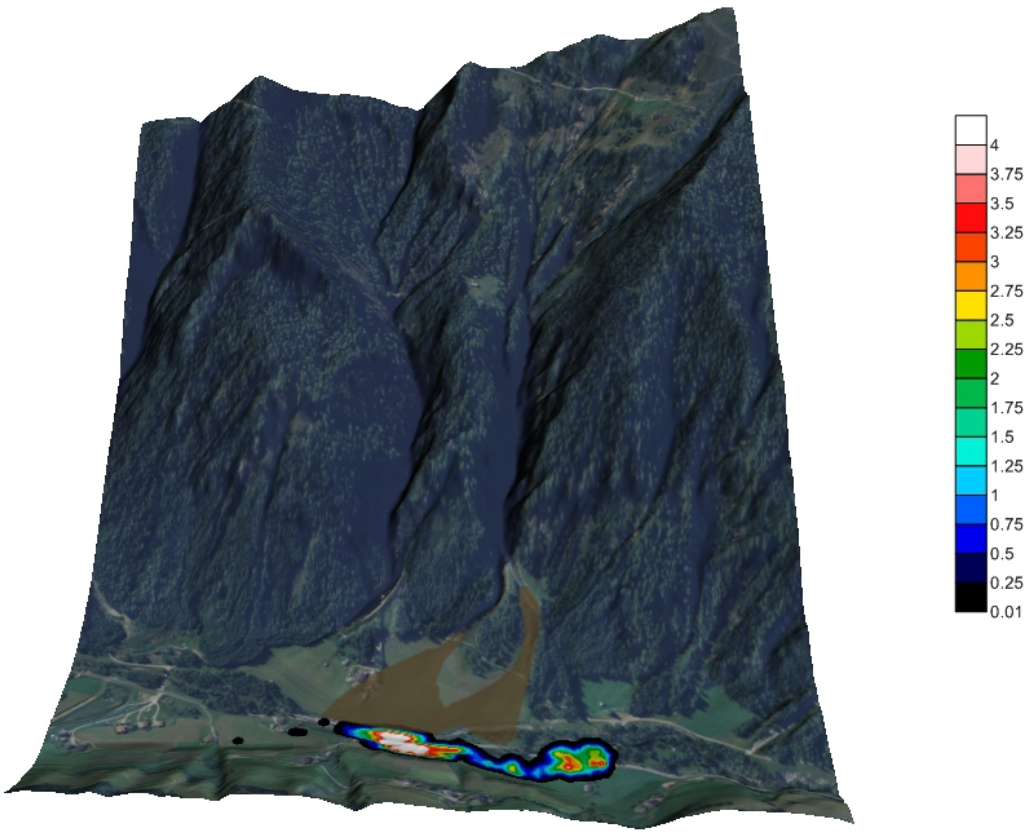

Figure 6.21 – Resulting deposits using $\phi_b = 12.5°$

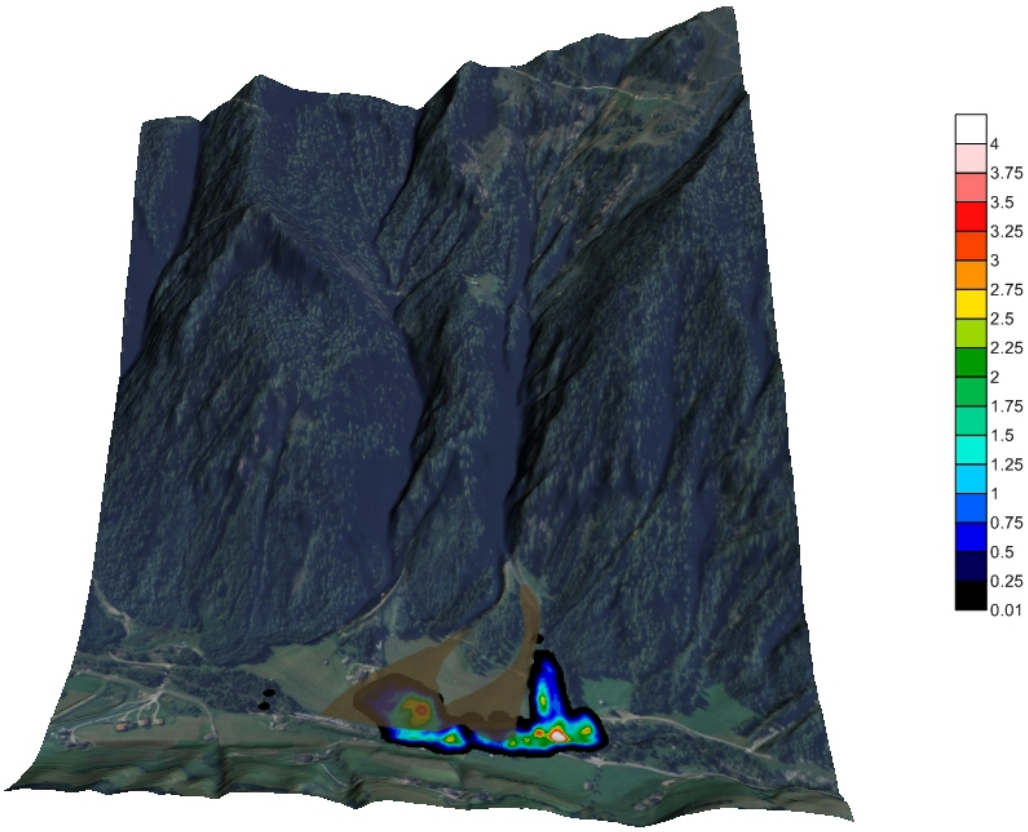

Figure 6.22 – Resulting deposits using $\phi_b = 15.0°$

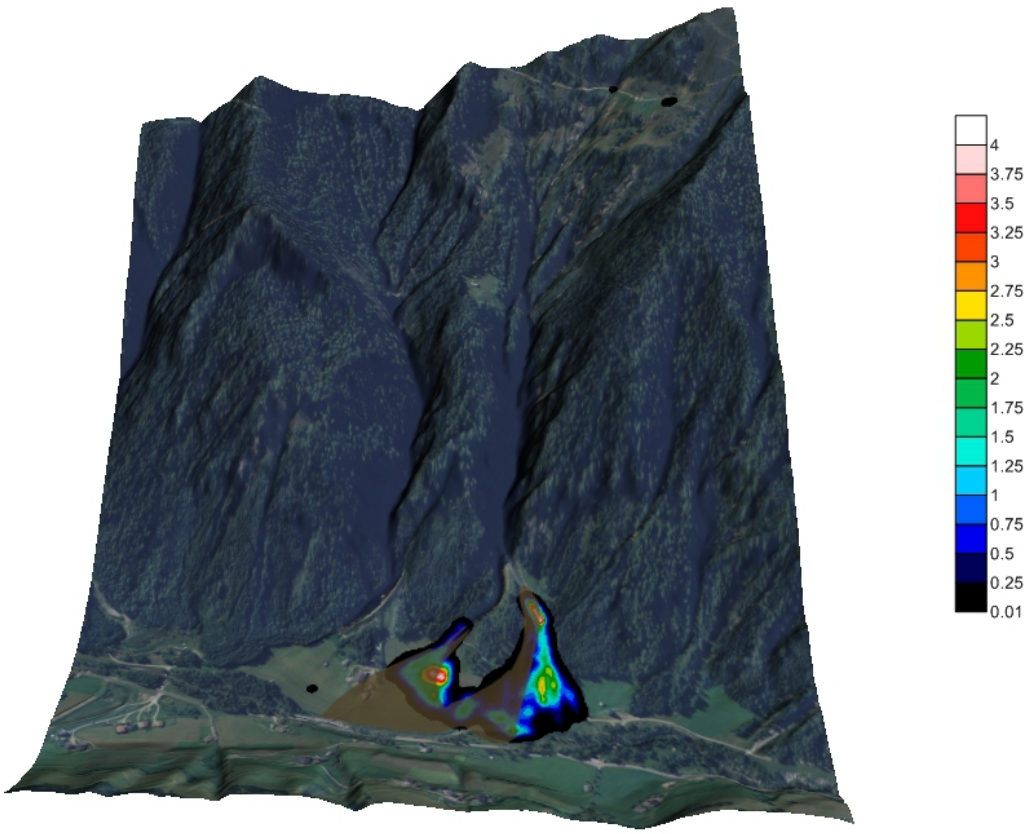

Figure 6.23 – Resulting deposits using $\phi_b = 17.5°$

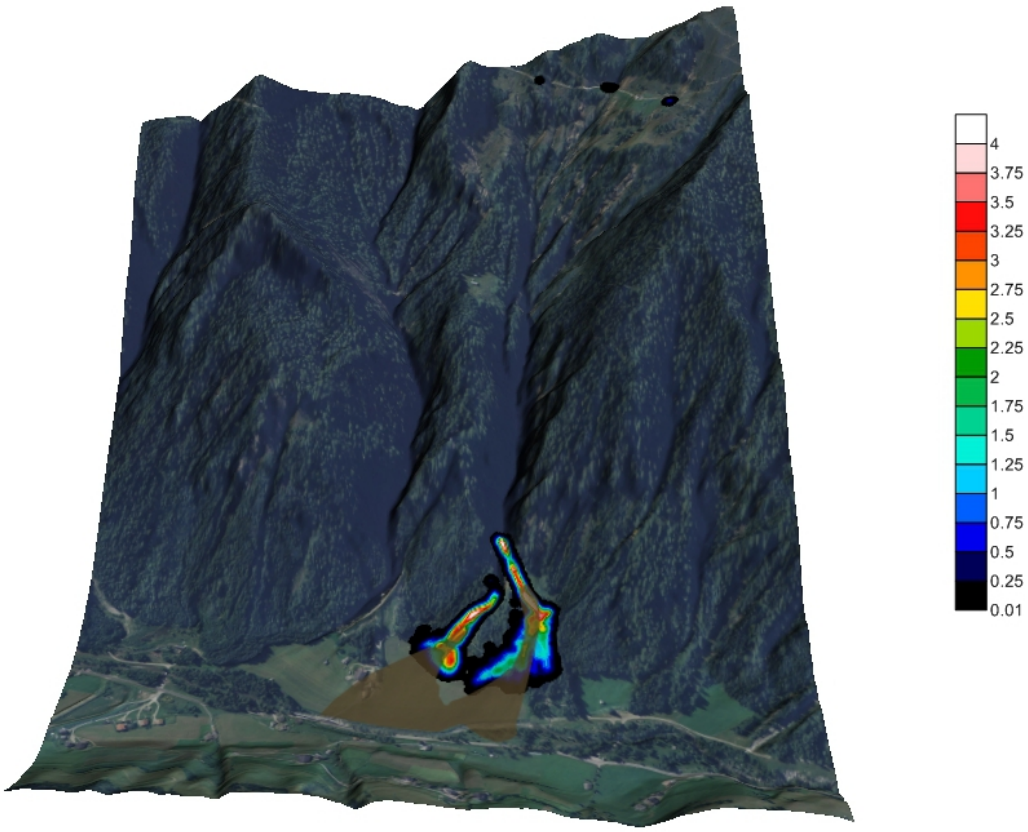

Figure 6.24 – Resulting deposits using $\phi_b = 20.0°$

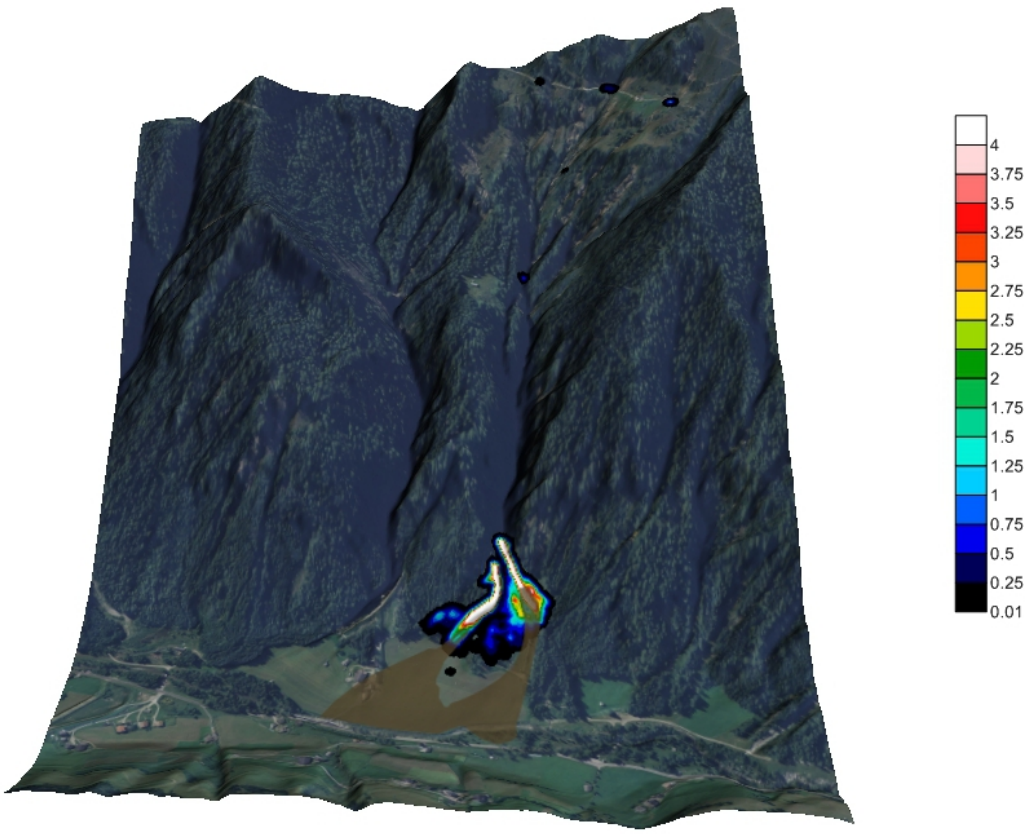

Figure 6.25 – Resulting deposits using $\phi_b = 22.5°$

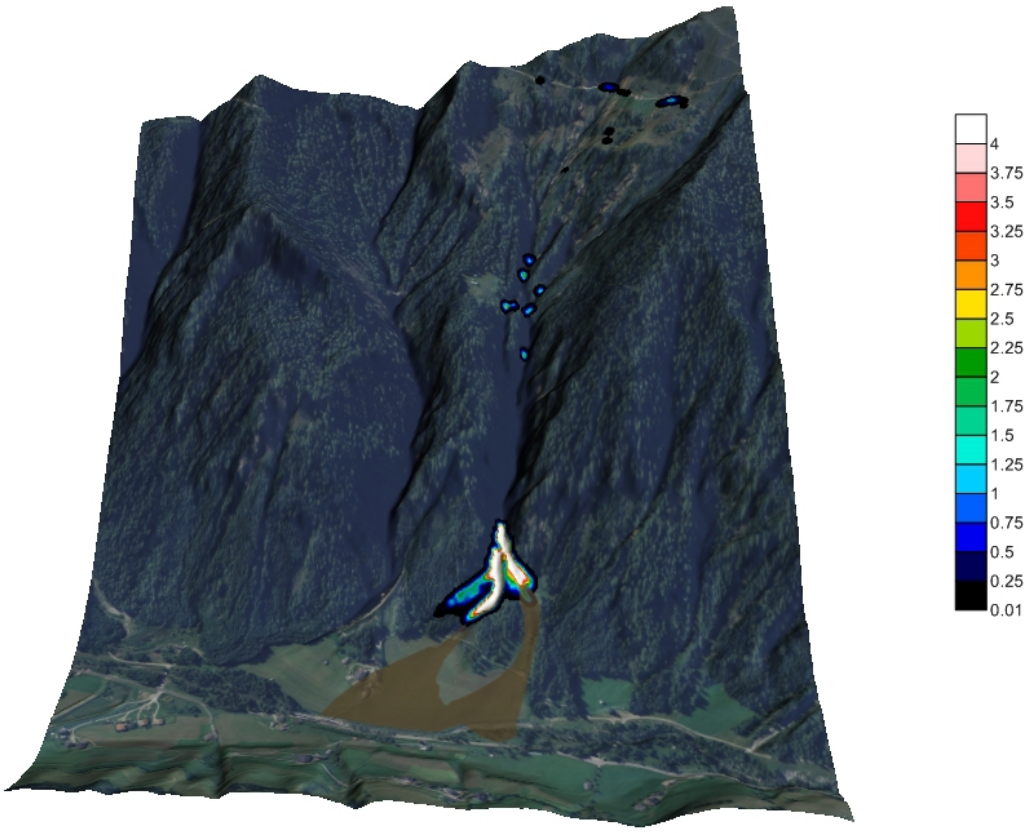

Figure 6.26 – Resulting deposits using $\phi_b = 25.0°$

6.6 Discussion

DAN3D was able to reproduce the "Seefeldbach" debris flow using the Voellmy rheology. The used friction coefficient $f = 0.1$ and turbulence coefficient $\xi = 500$ m/s^2 are the same as proposed by Ayotte and Hungr (2000) for rockfalls. Whether or not this set of parameters can be used in general, cannot be answered and is postponed to future investigations. The results show the high importance of the topography grid on the performance of the model. The debris flow follows all important topography features, fits the deposit area well and reproduces its heights well.

The model using the frictional rheology does not produce results as good as the models using the Voellmy rheology. The debris deposit is too lumped and does not have the proper shape. This can be explained by the lack of a velocity dependent basal shear resistance. The frictional rheology only uses the basal friction angle and pore water pressure for the calculation of the basal shear resistance. Compared to a model using the Voellmy rheology it leads to a lower flow resistance along the travel path and to a higher resistance in the

deposition zones. Therefore the movement stops more abruptly.

Chapter 7

Summary and conclusions

DAN3D is capable of modeling the major properties of a debris flow. The inhomogeneous debris gets simplified with an equivalent fluid concept whose stress state is described by the Rankine theory. This equivalent fluid can flow over a complex 3D terrain the interaction of which is described by a basal resistance rheology. This basal shear resistance mainly controls the velocity and behavior of the runout. Material entrainment can be included into the model. Its kinematic effect on the runout is described by the conservation of momentum and a continuous update of the debris volume.

The debris unit weight γ, the friction coefficient f, the turbulence coefficient ξ, the internal friction angle ϕ_i, the erosion rate E_s and the source volume V were varied in order to find out the influence on the results using a simplified terrain. The results which were compared where the maximum deposit height, runout length, deposit area, deposit volume, maximum velocity and mean velocity. Comparing the range of the results for each parameter set provided information to create correlations between the input parameters and the results.

It showed that the unit weight had a negligible or rather uncorrelated influence on the results and can therefore not be used to control the runout behavior. The friction coefficient has the biggest influence on the results. Increasing the friction coefficient by 100 % results in a 250 % heigher deposit, a 300 % shorter runout and a 300 % smaller deposit area. The turbulence coefficient has a smaller impact on the results. Increasing the turbulence coefficient by 100 % results in a 35 % lower deposit height, a 40 % longer runout an a 40 % bigger deposit area. The internal friction angle has an even smaller influence. It

mainly controls the deposit height, runout length and deposit area and has only small influence on the deposit volume and velocities. The erosion rate variation showed a linear correlation on the runout length and deposit volume . Increasing the erosion rate by 100 % results in a 100% longer runout and a 170% bigger deposit volume. It has a small influence on the deposit height and runout length and has an even smaller influence on the velocities. The last sensibility analysis was performed using varying source volumes. This showed a linear correlation between the deposit volume and smaller positive correlation on the deposit height, the runout lenght, the deposit area and the velocities. Increasing the source volume results in a faster runout which has a higher deposit, longer runout, bigger deposit area and bigger deposit volume.

In order to perform a runout simulation, a lot of information needs to be available. Depending whether the model performs a back-analysis or a prediction, different variables need to be evaluated. The major difference between a back-analysis and a prediction is that for a prediction the model parameters and debris source are unknown. Performing a back-analysis may evaluate the model parameters for the prediction of a future event. Using parameter sets of similar events could deliver the model parameters if there are no recorded events to be back-analyzed. Predicting the source volume is a more complex problem which can be solved using empirical or analytical methods. The correct assumption of the debris source is critical for a prediction and has the same importance as setting the proper model parameters.

The data of the "Seefeldbach" debris flow event could be transformed into the DAN3D grid files. Most information needed to be extracted from the on site photographs due to the lack of discrete source and deposit information, because the pre-event DEM was not accurate enough.

Both the Voellmy and friction rheologies were used to back-analyze this event. Best-fit results were generated using the Voellmy rheology with a friction coefficient of $f = 0.1$ and turbulence coefficient $\xi = 500$ m/s^2. Using the frictional rheology with the bulk friction angle $\phi_b = 15°$ produced the best-fit result for this rheology. Comparing both results shows that the Voellmy rheology is more capable to simulate this runout.

Errors in the debris deposits result from the usage of the post-event DEM. Neglecting this minor divergence, DAN3D is capable of simulating this debris flow event. It should

be pointed out, that the obtained results could be taken as a prediction for an event with the same source volume. According to the results of the simulations, an event similar to the 2002 event will most probably go over and damage the houses.

References

Abteilung11.6. CARG - Carta Geologica d'Italia 1:50.000, Autonome Provinz Bozen, Amt für Geologie und Baustoffprüfung, 2011. URL `http://www.provinz.bz.it/hochbau/projektierung/812.asp`.

Abteilung27. Digitale Unterlagen der Landeskartografie, Autonome Provinz Bozen, Amt für überörtliche Raumordnung, 2010. URL `http://www.provinz.bz.it/informatik/themen/landeskartografie.asp`.

Abteilung30. Ereignisdokumentation Südtirol, Autonome Provinz Bozen, Wasserschutzbauten, 2010. URL `http://www.provinz.bz.it/wasserschutzbauten`.

D. Ayotte and O. Hungr. Calibration of a runout prediction model for debris flows and avalanches. In *Proceedings 2nd International Conference on Debris Flows*, pages pp. 505–514, Taipei, 2000.

P. Brufau, P. Garcia-Navarro, P. Ghilardi, L. Natale, and F. Savi. 1d mathematical modelling of debris flow. *Journal of Hydraulic Research*, 38(6):pp.435–446, 2000.

J. Cepeda. The 2005 tate´s cairn debris flow: back-analysis, forward prediction and a sensitivity analysis. In *The 2007 International Forum on Landslide Disaster Management*, pages pp. 813–833, 2008.

D. Chan, N. Morgenstern, D. Tran, and X. Wang. Analysis of hong kong debris flow with an energy based model. In *The 2007 International Forum on Landslide Disaster Management*, pages pp. 835–855, 2008.

H. Chen and C.F. Lee. A dynamic model for rainfall-induced landslides on natural slopes. *Geomorphology*, 51:pp.269–288, 2003a.

H. Chen and C.F. Lee. A dynamic model for rainfall-induced landslides on natural slopes. *Geo*, 51:pp.269–288, 2003b.

R.P. Denlinger and R.M. Iverson. Flow of variably fluidized granular masses across three-dimensional terrain, 2. numerical predictions and experimental tests. *Journal of Geophysical Research*, 106(B1):pp.553–566, 2001.

R.P. Denlinger and R.M. Iverson. Granular avalanches across irregular three-dimensional terrain. *Journal of Geophysical Research*, 109:F01014, 2004.

Ken Ho and Victor Li. Proceedings of the 2007 international forum on landslide disaster management. volume II. Geotechnical Division, The Hong Kong Institution of Engineers, 2007.

M. Hürlimann, V. Medina, and A. Bateman. Application of 2d-finite volume code flat-model to landslide runout benchmarking exercises. In *The 2007 International Forum on Landslide Disaster Management*, pages pp. 933–943, 2008.

O. Hungr. A model for the runout analysis of rapid flow slides, debris flows, and avalanches. *Canadian Geotechnical Journal*, 32:pp.610–623, 1995.

O. Hungr. *DAN3D Interim instructions*, 2006. DAN3D package.

K. Hutter and S.B. Savage. Avalange dynamics: The motion of a finite mass of gravel down a mountain side. In *Proceedings of the 5th International Symposium on Landslides*, pages pp.691–697. Balkema A., Rotterdam, 1988.

M. Jakob, O. Hungr, and et. al. *Debris-flow Harzards and Related Phenomena.* Praxis Publishing, 2005.

J. Kwan and H.W. Sun. Benchmarking exercise on landslide mobility modelling - runout analyses using 3ddmm. In *The 2007 International Forum on Landslide Disaster Management*, pages pp. 945–966, 2008.

S. McDougal. *A new continuum dynamic model for the analysis of extremely rapid landslide motion across complex 3D terrain.* PhD thesis, The University of British Columbia, 2006.

P.J. McLellan and P.K. Kaiser. Application of a two-parameter model to rock avalanches in the mackenzine mountains. In *Proceedings of the 4th International Symposium on Landslides*, 1984.

V. Median, M. Hürlimann, and A. Bateman. Application of flatmodel, a 2d finite volume code, to debris flows in the northeastern part of the iberian peninsula. *Landslides*, 5: pp. 127–142, 2008.

D.R. Montgomery and W.E. Dietrich. A physically-based madel for the topographic control on shallow landsliding. *Water Resources Research*, 30:1153–1171, 1994.

J.S. O´Brien. Two-dimensional water flood and mudflow simulation. *Journal of Hydraulic Engineering*, 119(2):244–261, 1993.

R.T. Pack, D.G. Tarboton, and C.N. Goodwin. The sinmap approach to terrain stability mapping. In *Proceedings of 8th Congress of the Association of Engineering Geology*, volume 2, pages pp. 1157–1165, New York, 1998. American Society of Civil Engineers.

M. Pirulli. *Numerical Modelling of Landslide Runout, A Continuum Mechanics Approach.* PhD thesis, Politecnico di Torino, Italy, 2005.

M. Pirulli and C. Scavia. A set fo benchmark tests to assess the performance of a continuum mechanics depth-integrated model. In *The 2007 International Forum on Landslide Disaster Management*, pages pp. 1015–1042, 2008.

M. Pirulli, C. Scavia, and O. Hungr. Determination of rock avalanche run-out parameters through back analyses. In *Proceedings of the 9th International Symposium on Landslides*, pages pp. 1361–1366, Rio de Janeiro, 2004.

K. Sassa. Geotechnical model for the motion of landslides. In *Proceedings of the 5^{th} International Symposium on Landslides*, pages pp.37–55. Balkema A., Rotterdam, 1988.

S.B. Savage and K. Hutter. The motion of a finite mass of granular material down a rough incline. *Journal of Fluid Mechanics*, 199:pp.177–215, 1989.

R. Sosio, G.B. Crosta, and O. Hungr. Complete dynamic modeling calibration for the thurwieser rock avalanche (italian central alps). *Engineering Geology*, 100:pp. 11–26, 2008.

T. Takahashi. Mechanical characteristics of debris flow. *Journal of the Hydraulics Division of the American Society of Civil Engineers*, 104(HY8):pp.1153–1169, 1978.

T. Takahashi. Debris flow. International Association for Hydraulic Research monography. A.A. Balkema, 1991.

K. Terzaghi, R.B. Peck, and G. Mesri. *Soil mechanics in engineering practice.* Wiley Interscience, New York, 1967.

A. Voellmy. Über die zerstörungskraft von lawinen. *Schweizerische Bauzeitung*, 73:pp.212–285, 1955.

X. Wang. *Geotechnical Analysis of Flow Slides, Debris Flows, and Related Phenomena.* PhD thesis, University of Alberta, 2008.

List of Figures

List of Tables